mathematics

MDPI

Article

Analyzing the Dynamics of a Periodic Typhoid Fever Transmission Model with Imperfect Vaccination

Mohammed H. Alharbi [1,†], Fawaz K. Alalhareth [2,†] and Mahmoud A. Ibrahim [3,4,*,†]

[1] Department of Mathematics, College of Science, University of Jeddah, Jeddah 21589, Saudi Arabia
[2] Department of Mathematics, College of Arts & Sciences, Najran University, Najran 61441, Saudi Arabia
[3] Bolyai Institute, University of Szeged, Aradi vértanúk tere 1, 6720 Szeged, Hungary
[4] Department of Mathematics, Faculty of Science, Mansoura University, Mansoura 35516, Egypt
* Correspondence: mibrahim@math.u-szeged.hu or mahmoud_ali@mans.edu.eg
† These authors contributed equally to this work.

Abstract: We present a nonautonomous compartmental model that incorporates vaccination and accounts for the seasonal transmission of typhoid fever. The dynamics of the system are governed by the basic reproductive number $\mathcal{R}_0$. This demonstrates the global stability of the disease-free solution if $\mathcal{R}_0 < 1$. On the contrary, if $\mathcal{R}_0 > 1$, the disease persists and positive periodic solutions exist. Numerical simulations validate our theoretical findings. To accurately fit typhoid fever data in Taiwan from 2008 to 2023, we use the model and estimate its parameters using Latin hypercube sampling and least squares techniques. A sensitivity analysis reveals the significant influence of parameters such as infection rates on the reproduction number. Increasing vaccination coverage, despite challenges in developing countries, reduces typhoid cases. Accessible and highly effective vaccines play a critical role in suppressing the epidemic, outweighing concerns about the efficacy of the vaccine. Investigating possible parameter changes in Taiwan highlights the importance of monitoring and managing transmission rates to prevent recurring annual epidemics.

Keywords: typhoid fever; seasonal model; partially susceptible; reproduction numbers; global stability; periodic solutions; sensitivity analysis

MSC: 34C23; 34C25; 92D25; 92D30; 34C60; 37N25

Citation: Alharbi, M.H.; Alalhareth, F.K.; Ibrahim, M.A. Analyzing the Dynamics of a Periodic Typhoid Fever Transmission Model with Imperfect Vaccination. *Mathematics* **2023**, *11*, 3298. https://doi.org/10.3390/math11153298

Academic Editor: Davide Valenti

Received: 17 June 2023
Revised: 14 July 2023
Accepted: 25 July 2023
Published: 26 July 2023

1. Introduction

Typhoid fever, caused by the bacterium *Salmonella* Typhi, is a contagious disease prevalent in areas with limited resources and poor sanitation, significantly affecting public health through widespread disease and mortality. Typhoid fever can spread by contaminated food or water, poor sanitation, or close contact with infected individuals [1,2]. Symptoms include a persistent high fever, headache, weakness, stomach pain, and gastrointestinal problems. Patients may develop a skin rash in some cases, while critical cases can lead to severe consequences or fatality [3]. The global impact of typhoid fever is significant, particularly in resource-limited nations struggling with limited access to clean water and poor sanitation. The WHO (World Health Organization) estimates approximately 9 million cases and 110,000 deaths annually worldwide. Although the disease is controlled in developed countries, it persists as an endemic disease in numerous regions around the world. South Asia, including India, Pakistan, and Bangladesh, experiences an exceptionally high impact of this disease [3–5].

Although prevention programs such as improved sanitation and food hygiene are crucial, it often takes time for these programs to show improvements in most areas affected by typhoid fever. Furthermore, the persistence of the disease can be attributed to bacterial resistance to antibiotics, which are commonly used for treatment, and the presence of multiple Salmonella strains [6–8]. However, typhoid vaccination remains an indispensable

measure of disease control, particularly during outbreaks or in endemic environments. The World Health Organization (WHO) has recommended two types of typhoid vaccines, the Vi Polysaccharide vaccine and the Ty21a oral vaccine, since 2008. However, obtaining typhoid vaccines in developing countries can be limited and challenging [9].

Mathematical models have been extensively used to investigate the transmission dynamics of typhoid fever and evaluate the effectiveness of various prevention programs. Previous studies have employed these models to focus on different aspects of disease transmission. Some models specifically address direct human-to-human transmission [10–12], while others incorporate the contribution of indirect transmission through contaminated food and water [13,14]. Some comprehensive models consider both direct and indirect modes of transmission [15–17], providing a more complete understanding of the spread of typhoid fever. These models have been instrumental in evaluating the impact of interventions such as disease treatment [14,18], sanitation measures [19,20], education campaigns [21,22], and media coverage [23] on preventing typhoid outbreaks. The findings of these mathematical models contribute to the development of effective strategies for the control and prevention of typhoid fever.

In their study, Musa et al. [22] developed an epidemic model to examine the dynamics of the transmission of typhoid fever and to evaluate the effectiveness of public health education programs in reducing its pathogenesis. The model was calibrated using data from Taiwan and China for typhoid fever. Through a mathematical analysis, they determined the stability conditions for the disease-free and endemic equilibrium and identified crucial parameters to control typhoid fever. Furthermore, they employed a wavelet analysis to detect significant periodic patterns in outbreaks of typhoid fever. Pitzer et al. [24] introduced a mathematical model to investigate the transmission dynamics of typhoid fever and assess the effects of vaccination, including direct and indirect impacts such as herd immunity. Their findings showed that although typhoid vaccination could provide indirect short-term protection and reduce disease incidence, complete elimination of the disease was unlikely to be achieved by vaccination alone. Edward et al. [19] developed a mathematical model to evaluate the effect of direct and indirect transmissions of typhoid fever, taking into account various interventions such as vaccination coverage, treatment, and water sanitation. The results of their study demonstrated the crucial role of these interventions in reducing the outbreak when promoted within the community. In addition, minimizing contact with typhoid patients and preventing the contamination of water sources with feces were identified as crucial measures in preventing typhoid outbreaks. In [25], the authors established a mathematical model that studied the dynamics of the transmission of typhoid fever. Their model incorporated a non-integer-order derivative and considered vaccination as a control measure. The stability of equilibrium points was analyzed, revealing that vaccination effectively reduced the spread of the disease. The study also conducted a sensitivity analysis to identify important parameters and validate the findings through numerical simulations. In a study by Sinan et al. [26], the dynamical model of typhoid fever was modeled and numerically solved. Local and global stability analyses were performed, showing that the model exhibited stability at both endemic and disease-free equilibrium points. Numerical solutions were obtained using the Adams–Bashforth method, and graphical representations supported the results. A recent study by Abboubakar and Racke [27] examined an autonomous model designed to prevent typhoid fever. The model took into account multiple control mechanisms, including an imperfect vaccine, hygiene practices, and therapeutic measures. Using clinical data from Mbandjock, Cameroon, the study explored the impact of these control mechanisms. The findings indicated that effective control of typhoid fever required a combination of measures, such as large-scale immunization campaigns, environmental sanitation, and appropriate therapeutic interventions.

The value of mathematical models in comprehending the transmission dynamics of typhoid fever and influencing the formulation of public health interventions aimed at preventing and controlling the disease is underscored by these studies. In line with this,

our study presents a nonautonomous mathematical model that explores the transmission dynamics of typhoid fever with vaccination in periodic environmental changes. We expand on the existing model proposed by [27] by incorporating the temporal periodicity of the environment, mainly including seasonal fluctuations in transmission rates that are correlated with rainfall patterns. Furthermore, we acknowledge that the previous model neglected typhoid transmission through direct human-to-human contact. In our model, we take this aspect into account and recognize that direct human-to-human transmission plays a significant role in the overall spread of the disease. We formulate the basic reproduction number $\mathcal{R}_0$ for the periodic model to demonstrate its global stability, as well as the existence of positive periodic solutions, which depend on the value of $\mathcal{R}_0$. Our focus is on using our model to investigate the dynamics of the transmission of typhoid fever during the outbreak that occurred in Taiwan from 2008 to 2023. We calibrate our model using real data from Taiwan and estimate several parameters. Subsequently, we conduct a sensitivity analysis to identify the model parameters that significantly contribute to the transmission of the disease among the human community. This analysis involves computing sensitivity indices. Specifically, our objective is to examine the effect of imperfect vaccination on the transmission of the disease and to provide predictions for the estimated number of new cases of typhoid. In addition, we present numerical simulations to validate and support the analytical findings.

The article is structured into different sections. It starts with Section 2, which comprehensively explains the proposed model. In Section 3, the computation of $\mathcal{R}_0$ and a detailed analysis of the global dynamics in relation to $\mathcal{R}_0$ are presented. Section 4 includes the model calibration, sensitivity analysis, and prediction. Finally, Section 5 includes the findings and results obtained from numerical simulations.

2. Seasonal Typhoid Fever Model

To investigate the dynamics of typhoid fever, we categorized the human population into six distinct compartments based on their clinical status. These compartments included susceptible ($S(t)$), vaccinated ($V(t)$), exposed ($E(t)$), asymptomatic infectious or carriers ($C(t)$), symptomatic infectious ($I(t)$), and recovered ($R(t)$). At any given time t, the total size of the human population is represented by $N(t)$, which is equal to the sum of individuals in each compartment: $N(t) = S(t) + V(t) + E(t) + C(t) + I(t) + R(t)$. Furthermore, we used the compartment $B(t)$ to represent the density of bacteria in the environment. The model is visually represented in Figure 1.

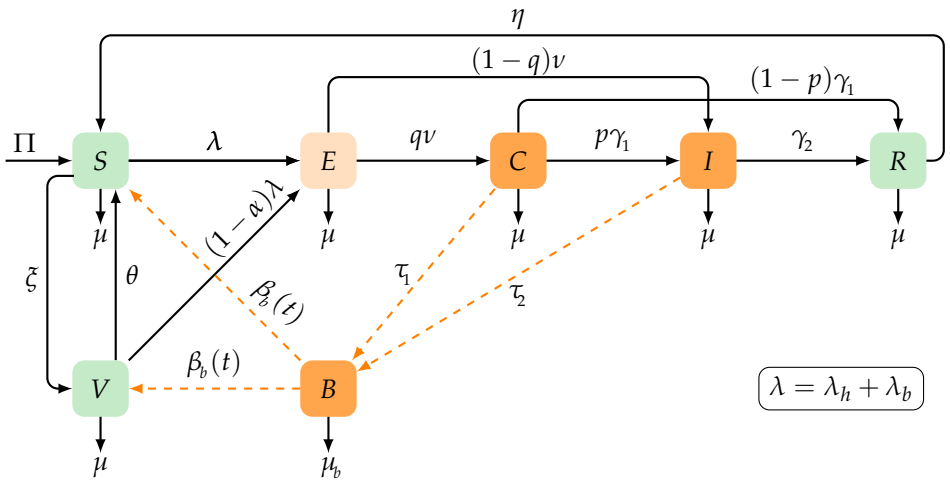

Figure 1. Transmission diagram of the typhoid model (1).

The equations for our model are as follows:

$$\begin{aligned}
S'(t) &= \Pi + \eta R(t) + \theta V(t) - \big(\lambda_h(t) + \lambda_b(t)\big)S(t) - (\xi + \mu)S(t),\\
V'(t) &= \xi S(t) - (1-\alpha)\big(\lambda_h(t) + \lambda_b(t)\big)V(t) - (\theta + \mu)V(t),\\
E'(t) &= \big(\lambda_h(t) + \lambda_b(t)\big)\big(S(t) + (1-\alpha)V(t)\big) - (\nu + \mu)E(t),\\
C'(t) &= q\nu E(t) - (\gamma_1 + \mu)C(t),\\
I'(t) &= (1-q)\nu E(t) + p\gamma_1 C(t) - (\gamma_2 + \mu + \delta)I(t),\\
R'(t) &= (1-p)\gamma_1 C(t) + \gamma_2 I(t) - (\eta + \mu)R(t),\\
B'(t) &= \tau_1 C(t) + \tau_2 I(t) - \mu_b B(t),
\end{aligned} \tag{1}$$

where $\lambda_h(t) = \beta_1 C(t) + \beta_2 I(t)$ and $\lambda_b(t) = \beta_b(t)B(t)$ are mass action incidences, following the references [27–29]. The rate of infection from the environment to humans is denoted by $\beta_b(t)$ in our model. We assumed that $\beta_b(t)$ was a continuous positive function with a period of T to capture seasonal variations in disease transmission, as stated in Equation (1).

We use the symbols Π and μ to represent the recruitment rate of humans and the natural death rate, respectively. Immunity to the vaccine is temporary, and its waning rate is indicated by θ. Individuals who have received the vaccine and are susceptible move to the vaccinated compartment V at a rate of ξ. When susceptible individuals are infected, they move to the exposed class ($E(t)$), where they remain for a period of time $1/\nu$. The infection rate for susceptible individuals is $\lambda_h(t) + \lambda_b(t)$, which can occur through human-to-human transmission or environment-to-human transmission. Recent research [30] suggests that the efficacy of typhoid fever vaccines is less than 95%, indicating that the vaccine is not completely perfect. Therefore, there exists the possibility that vaccinated individuals become infected at a rate of $(1-\alpha)(\lambda_h(t) + \lambda_b(t))$, where α represents the efficacy of the vaccine. A value of $\alpha = 0$ means that the vaccine does not provide protection, while a value of $\alpha = 1$ indicates a perfect vaccine ($0 < \alpha < 1$). Individuals in the exposed E class develop asymptomatic infection and become carriers C at a rate of $q\nu$. The value of q indicates the probability that an individual transitions from a latent state to a carrier C or symptomatic infection (I) with a frequency of $(1-q)\nu$. Individuals in the carrier class C move to the infectious symptomatic class with a frequency of $p\gamma_1$. Here, p denotes the likelihood that an asymptomatic individual becomes symptomatic, while γ_1 represents the rate at which carriers develop natural immunity. Alternatively, carriers can recover at a rate of $(1-p)\gamma_1$. Individuals who are symptomatic and infectious recover at a consistent rate of γ_2 or may experience disease-induced death with a rate of δ. Following the infection, individuals who have recovered experience a gradual loss of immunity at a rate of η. To provide a comprehensive summary of our model, we list the parameters of our model in Table 1.

Table 1. Summary of the parameters and notations of model (1).

Parameters	Description
Π	Human birth rate
μ	Natural mortality rate
β_1, β_2	Human-to-human transmission rates
$\beta_b(t)$	Environment to human infection rate
τ_1, τ_2	Bacteria excretion (carriers, infectious)
γ_1, γ_2	Recovery rates
ν	Rate of progression to carriers
q	Probability of exposed group E transitioning into carriers C
p	Probability of carriers C to become infected I
δ	Disease-induced mortality

Table 1. *Cont.*

Parameters	Description
η	Rate of transition from recovered to susceptible classes
α	Vaccine efficacy
θ	Vaccination waning rate
ξ	Vaccination rate
μ_b	Bacterial decay rate

2.1. Basic Properties

Given non-negative initial values, any solution to system (1) is also non-negative. Therefore, we first discuss the limits or bounds of the solution of (1). For ease of analysis, we define

$$\big(S(0), V(0), E(0), C(0), I(0), R(0), B(0)\big) = \big(S^0, V^0, E^0, C^0, I^0, R^0, B^0\big) \in \mathbb{R}^7_+,$$

where $\mathbb{R}_+ := [0, \infty)$. Given a positive initial condition $\big(S^0, V^0, E^0, C^0, I^0, R^0, B^0\big) \in \mathbb{R}^7_+$, the human subsystem of system (1) yields $N(t)$ as a solution to the differential equation

$$N'(t) = \Pi - \mu N(t) - \delta I(t) \leq \Pi - \mu N(t). \tag{2}$$

As a consequence, we have

$$\limsup_{t\to\infty} N(t) \leq \frac{\Pi}{\mu}.$$

Under the assumption of no disease within the population, (2) possesses a single globally asymptotically stable equilibrium Π/μ, and $N(t)$ remains bounded. Using the inequality $I(t) \leq N(t) \leq \Pi/\mu$ and $C(t) \leq N(t) \leq \Pi/\mu$ derived previously, we can deduce from the last equation in (1) the following result:

$$B^{'}(t) \leq \frac{(\tau_1 + \tau_2)\Pi}{\mu} - \mu_b B(t). \tag{3}$$

After solving differential Equation (3), we obtain $B(t) \leq \frac{(\tau_1+\tau_2)\Pi}{\mu} + B^0 e^{-\mu_b t}$, which implies that B is non-negative. Taking the limit as $t \to \infty$, we have

$$\limsup_{t\to\infty} B(t) \leq \frac{\gamma(\tau_1 + \tau_2)\Pi}{\mu_b \mu},$$

and thus $B(t)$ is also bounded. Therefore, the solutions of model (1) are bounded and non-negative within the region:

$$\Omega := \left\{(S, V, E, C, I, R, B) \in \mathbb{R}^7_+ : \ N \leqslant \frac{\Pi}{\mu}, \ B \leqslant \frac{\gamma(\tau_1 + \tau_2)\Pi}{\mu_b \mu}\right\}.$$

The above analysis leads to the following conclusion:

Proposition 1. *If the initial values of system* (1) *are positive, i.e.,* $\big(S^0, V^0, E^0, C^0, I^0, R^0, B^0\big) \in \mathbb{R}^7_+$, *then the solution of the system,* $\big(S(t), V(t), E(t), C(t), I(t), R(t), B(t)\big)$, *remains positive for all* $t > 0$, *implying that the system is positively invariant with respect to the region* Ω.

Proof. To demonstrate the non-negativity of the solutions of system (1), we can prove that for $\big(S^0, V^0, E^0, C^0, I^0, R^0, B^0\big) \in \mathbb{R}^7_+$, the solution of system (1), $(S(t), V(t), E(t), C(t), I(t), R(t))$ remains greater than or equal to zero for all $t > 0$. Let us define

$$m(t) = \min\{S(t), V(t), E(t), C(t), I(t), R(t)\}, \ \forall t > 0.$$

Since $m(0) > 0$, we can assume the existence of a time point $t_1 > 0$ where $m(t_1) = 0$ and that $m(t) > 0$ for all $t \in [0, t_1)$. Assuming $m(t_1) = S(t_1)$, the first equation of system (1) implies the inequality

$$S'(t) \geq -\big(\lambda_h(t) + \lambda_b(t) + \xi + \mu\big)S(t), \quad \forall t \in [0, t_1].$$

Then,

$$0 = S(t_1) \geq S^0 e^{-\int_0^{t_1} \left(\lambda_h(t)+\lambda_b(t)+\xi+\mu\right) ds} > 0.$$

This contradiction arises from the impossibility of having negative values for $S(t)$ for any $t > 0$. Similarly, we can reach a similar conclusion with regard to $V(t)$ using analogous arguments.

Consider the last four compartments of the human subsystem of (1). We assume that there exists a minimum time value of $t > 0$ at which one of the compartments, namely, $E(t)$, $C(t)$, $I(t)$, or $R(t)$, becomes zero. Without loss of generality, assume that this compartment is $E(t)$.

If $m(t_1) = E(t_1)$, then from the fourth equation of (1), we have $I(t) \geq 0$, $C(t) \geq 0$, $B(t) \geq 0$, $V(t) \geq 0$, and $S(t) \geq 0$ for all $t \in [0, t_1]$. Thus, we obtain

$$E'(t) \geq -(\nu + \mu)E(t), \quad \forall t \in [0, t_1].$$

Hence,

$$0 = E(t_1) \geq E^0 e^{-(\nu+\mu)t_1} > 0,$$

which leads to a contradiction. Similarly, if $m(t_1) = C(t_1)$, $m(t_1) = I(t_1)$, or $m(t_1) = R(t_1)$, then a similar contradictory conclusion can be reached. Therefore, we conclude that $S(t) \geq 0$, $V(t) \geq 0$, $E(t) \geq 0$, $C(t) \geq 0$, $I(t) \geq 0$, and $R(t) \geq 0$ for all $t > 0$. Furthermore, equality is present if the initial conditions are set to zero.

Equation (2) allows us to express $N(t)$ as $N^0 e^{-\mu t} + \frac{\Pi}{\mu}(1 - e^{-\mu t})$, where $N^0 = S^0 + V^0 + E^0 + C^0 + I^0 + R^0$. Therefore, $N(t)$ is bounded for all $t \geq 0$, and we have $\limsup_{t\to\infty} N(t) = \frac{\Pi}{\mu}$. Additionally, $\limsup_{t\to\infty} B(t) \leq \frac{(\tau_1+\tau_2)\Pi}{\mu_b \mu}$, which implies that $S(t)$, $V(t)$, $E(t)$, $C(t)$, $I(t)$, $R(t)$, and $B(t)$ are all bounded for all $t > 0$. Therefore, the proof is complete. □

2.2. Disease-Free Solution

The disease-free solution of (1) is provided when there is no presence of disease by solving the following system

$$\begin{aligned} 0 &= \Pi + \theta V^* - (\xi + \mu)S^*, \\ 0 &= \xi S^* - (\theta + \mu)V^*; \end{aligned}$$

therefore, system (1) has a single disease-free solution, denoted as

$$P^* = \big(S^*, V^*, E^*, C^*, I^*, R^*, B^*\big) = \left(\frac{(\theta+\mu)\Pi}{\mu(\xi+\theta+\mu)}, \frac{\xi\Pi}{\mu(\xi+\theta+\mu)}, 0, 0, 0, 0, 0\right),$$

and it is always feasible.

3. Threshold Dynamics

This section aims to establish the stability of the disease-free periodic solution P^* globally and to prove that the disease dies when $\mathcal{R}_0 < 1$. However, when $\mathcal{R}_0$ is greater than 1, we demonstrate the existence of a positive periodic solution for (1) and the persistence of the disease. First, we obtain the basic reproduction number $\mathcal{R}_0$ utilizing the approach outlined in the work of Wang and Zhao [31].

3.1. Basic Reproduction Number

Let $\mathcal{X} = (E, C, I, B, S, V, R)^T$ where E, C, I, and B represent the infected classes, and S, V, and R are the uninfected classes with

$$\mathcal{F}(t, \mathcal{X}(t)) = \begin{bmatrix} \left(\lambda_h(t)+\lambda_b(t)\right)\left(S(t)+(1-\alpha)V(t)\right) \\ 0 \\ 0 \\ 0 \\ 0 \\ 0 \\ 0 \end{bmatrix},$$

$$\mathcal{V}^-(t, \mathcal{X}(t)) = \begin{bmatrix} (\nu+\mu)E(t) \\ (\gamma_1+\mu)C(t) \\ (\gamma_2+\mu+\delta)I(t) \\ \mu_b B(t) \\ \left(\lambda_h(t)+\lambda_b(t)\right)S(t)+(\xi+\mu)S(t) \\ (1-\alpha)\left(\lambda_h(t)+\lambda_b(t)\right)V(t)+(\theta+\mu)V(t) \\ (\eta+\mu)R(t) \end{bmatrix}, \quad \mathcal{V}^+(t, \mathcal{X}(t)) = \begin{bmatrix} 0 \\ q\nu E(t) \\ (1-q)\nu E(t)+p\gamma_1 C(t) \\ \tau_1 C(t)+\tau_2 I(t) \\ \Pi+\eta R(t)+\theta V(t) \\ \xi S(t) \\ (1-p)\gamma_1 C(t)+\gamma_2 I(t) \end{bmatrix}.$$

The following nonautonomous equation

$$\mathcal{X}'(t) = \mathcal{F}(t, \mathcal{X}(t)) - \mathcal{V}(t, \mathcal{X}(t)), \tag{4}$$

is equivalent to system (1), where $\mathcal{V}(t, \mathcal{X}(t)) = \mathcal{V}^-(t, \mathcal{X}(t)) - \mathcal{V}^+(t, \mathcal{X}(t))$. The disease-free solution of (4) is $\mathcal{X}^* = (0, 0, 0, 0, 0, 0, S^*, V^*, 0)$. To compute the 4×4 matrix functions $F(t)$ and $V(t)$, where $F(t)$ is defined as $\left(\frac{\partial \mathcal{F}_i(t, \mathcal{X}^*)}{\partial \mathcal{X}_j}\right)_{1 \leqslant i,j \leqslant 4}$ and $V(t)$ is defined as $\left(\frac{\partial \mathcal{V}_i(t, \mathcal{X}^*)}{\partial \mathcal{X}_j}\right)_{1 \leqslant i,j \leqslant 4}$, we need to find the entries of $F(t)$ and $V(t)$, which are given by:

$$F(t) = \begin{bmatrix} 0 & \beta_1\left(S^* + (1-\alpha)V^*\right) & \beta_2\left(S^* + (1-\alpha)V^*\right) & \beta_b(t)\left(S^* + (1-\alpha)V^*\right) \\ 0 & 0 & 0 & 0 \\ 0 & 0 & 0 & 0 \\ 0 & 0 & 0 & 0 \end{bmatrix},$$

and

$$V(t) = \begin{bmatrix} \nu + \mu & 0 & 0 & 0 \\ -q\nu & \gamma_1 + \mu & 0 & 0 \\ -(1-q)\nu & -p\gamma_1 & \gamma_2 + \mu + \delta & 0 \\ 0 & -\tau_1 & -\tau_2 & \mu_b \end{bmatrix}.$$

Consider the initial value problem:

$$\mathcal{Z}'(t_1, t_2) = \mathcal{F}(t_1, \mathcal{Z}(t_1, t_2)), \qquad \mathcal{Z}(t_2, t_2) = \mathcal{I}_4, \tag{5}$$

where $\mathcal{F}(t_1, \mathcal{Z}(t_1, t_2)) = -V(t)\mathcal{Z}(t_1, t_2)$ is a vector function and $\mathcal{I}_4$ is the 4×4 identity matrix. Suppose $\mathcal{Z}(t_1, t_2)$ is the matrix solution of (5), where $t_1 \geqslant t_2$. We make the assumption that $\mathcal{C}_T$ is an ordered Banach space consisting of functions that are periodic with a period of T and map from $\mathbb{R}$ to $\mathbb{R}^4$, equipped with the standard maximum norm $\|\cdot\|_\infty$. We also define the positive cone $\mathcal{C}_T^+$ as the set of all functions $\phi \in \mathcal{C}_T$ such that $\phi(t) \geqslant 0$ for all $t \in \mathbb{R}$.

As described in [31], we establish the basic reproduction number of (1), denoted by $\mathcal{R}_0$. It is determined by calculating the spectral radius of the linear next infection operator $\mathcal{K}: \mathcal{C}_T \to \mathcal{C}_T$, which is defined in the following manner:

$$(\mathcal{K}\phi)(t) = \int_0^\infty \mathcal{Z}(t, t-a)F(t-a)\phi(t-a)\,da, \qquad \forall t \in \mathbb{R},\ \phi \in \mathcal{C}_T;$$

therefore, $\mathcal{R}_0 := \rho(\mathcal{K})$. Referring to Theorems 2.1 and 2.2 in [31], we can derive the following result:

Theorem 1 ([31], Theorem 2.2)**.** *Let $\Phi_{F-V}(t)$ represent the monodromy matrix of the T-periodic linear system $x' = (F(t) - V(t))x$. The following statements are valid:*

1. $\rho(\Phi_{F-V}(T)) = 1$ *if and only if* $\mathcal{R}_0 = 1$;
2. $\rho(\Phi_{F-V}(T)) < 1 (> 1)$ *if and only if* $\mathcal{R}_0 < 1 (> 1)$.

3.2. Local Stability of P^*

Based on the previous discussion, the following theorem focuses on the local stability of the unique disease-free solution P^* of system (1):

Theorem 2. *If $\mathcal{R}_0 < 1$, the disease-free solution P^* of system (1) is locally asymptotically stable and unstable if $\mathcal{R}_0 > 1$.*

Proof. The matrix that represents the Jacobian of Equation (1) when evaluated at P^* can be expressed as:

$$J(t) = \begin{bmatrix} F(t) - V(t) & 0 \\ A(t) & B \end{bmatrix},$$

where

$$A(t) = \begin{bmatrix} 0 & -\beta_1 S^* & -\beta_2 S^* & -\beta_b(t) S^* \\ 0 & -(1-\alpha)\beta_1 V^* & -(1-\alpha)\beta_2 V^* & -(1-\alpha)\beta_b(t) V^* \\ 0 & (1-p)\gamma_1 & \gamma_2 & 0 \end{bmatrix},$$

and

$$B = \begin{bmatrix} -\xi - \mu & \theta & \eta \\ \xi & -\theta - \mu & 0 \\ 0 & 0 & -\eta - \mu \end{bmatrix}.$$

The matrix B is constant and has negative eigenvalues $\lambda_{1,2,3} = -\xi - \mu, -\theta - \mu, -\eta - \mu$. Consequently, $\rho(\Phi_B) < 1$ due to the negativity of its eigenvalues. Thus, the stability of P^* is based on the value of $\rho(\Phi_{F-V}(T))$ as stated in [32]. Accordingly, if $\rho(\Phi_{F-V}(T)) < 1$, then P^* is LAS, otherwise, it is unstable. This concludes the proof by invoking Theorem 1. □

3.3. Global Stability of P^*

Theorem 3. *The disease-free periodic solution P^* of Equation (1) exhibits a global asymptotic stability when $\mathcal{R}_0 < 1$.*

Proof. Starting from the first equation of system (1), we obtain:

$$\begin{aligned} S'(t) &= \Pi + \eta R(t) + \theta V(t) - \big(\lambda_h(t) + \lambda_b(t)\big) S(t) - (\xi + \mu) S(t), \\ V'(t) &= \xi S(t) - (1-\alpha)\big(\lambda_h(t) + \lambda_b(t)\big) V(t) - (\theta + \mu) V(t). \end{aligned}$$

Since $C(t) \geq 0$, $I(t) \geq 0$, and $B(t) \geq 0$, as shown in Proposition 1, we can deduce the following inequalities:

$$\begin{aligned} S'(t) &\leq \Pi + \eta R(t) + \theta V(t) - (\xi + \mu) S(t), \\ V'(t) &\leq \xi S(t) - (\theta + \mu) V(t). \end{aligned}$$

These inequalities indicate that

$$\begin{aligned} \limsup_{t \to \infty} S(t) &\leq \frac{\Pi + \eta R^* + \theta V^*}{\xi + \mu} = \frac{(\theta + \mu)\Pi}{\mu(\xi + \theta + \mu)} = S^*, \\ \limsup_{t \to \infty} V(t) &\leq \frac{\xi S^*}{\theta + \mu} = \frac{\xi \Pi}{\mu(\xi + \theta + \mu)} = V^*. \end{aligned}$$

Therefore, for any positive value of ε, there exists a time point t_1 greater than zero such that for all t exceeding t_1, both $S(t)$ and $V(t)$ are less than or equal to $S^* + \varepsilon$ and $V^* + \varepsilon$, respectively.

By considering system (1), we can derive the following expression for $t > t_1$:

$$\begin{aligned}
E^{'}(t) &\leq \big(\lambda_h(t) + \lambda_b(t)\big)\big(S^* + \varepsilon + (1-\alpha)(V^* + \varepsilon)\big) - (\nu + \mu)E(t),\\
C^{'}(t) &\leq q\nu E(t) - (\gamma_1 + \mu)C(t),\\
I^{'}(t) &\leq (1-q)\nu E(t) + p\gamma_1 C(t) - (\gamma_2 + \mu + \delta)I(t),\\
B^{'}(t) &\leq \tau_1 C(t) + \tau_2 I(t) - \mu_b B(t),
\end{aligned}$$

and using the following comparison system

$$\begin{aligned}
E^{'}(t) &= \big(\lambda_h(t) + \lambda_b(t)\big)\big(S^* + \varepsilon + (1-\alpha)(V^* + \varepsilon)\big) - (\nu + \mu)E(t),\\
C^{'}(t) &= q\nu E(t) - (\gamma_1 + \mu)C(t),\\
I^{'}(t) &= (1-q)\nu E(t) + p\gamma_1 C(t) - (\gamma_2 + \mu + \delta)I(t),\\
B^{'}(t) &= \tau_1 C(t) + \tau_2 I(t) - \mu_b B(t),
\end{aligned} \tag{6}$$

the system of Equation (6) can be given in the following alternative form:

$$\frac{\mathrm{d}Y(t)}{\mathrm{d}t} = \big(F(t) - V(t) + \varepsilon M(t)\big)Y(t), \tag{7}$$

where $Y(t) = \big(E(t), C(t), I(t), B(t)\big)$ and the matrix function $M(t)$ given by

$$M(t) = \begin{bmatrix} 0 & \beta_1(2-\alpha) & \beta_2(2-\alpha) & \beta_b(t)(2-\alpha) \\ 0 & 0 & 0 & 0 \\ 0 & 0 & 0 & 0 \\ 0 & 0 & 0 & 0 \end{bmatrix}. \tag{8}$$

According to Theorem 2, the stability of P^* depends on the value of $\mathcal{R}_0$. Specifically, if $\mathcal{R}_0 > 1$, then P^* is unstable. On the contrary, if $\mathcal{R}_0 < 1$, P^* is locally asymptotically stable. Hence, it suffices to demonstrate that when $\mathcal{R}_0 < 1$, P^* is globally attractive. Theorem 1 indicates that $\mathcal{R}_0 < 1$ when $\rho(\Phi_{F-V}(T)) < 1$. As $\rho(\Phi_{F-V}(T))$ is a continuous function, it is possible to select a small positive ε such that $\rho(\Phi_{F-V+\varepsilon M}(T)) < 1$.

Based on Lemma 2.1 in [33], we can find a positive $p(t)$ with a period of T such that $Y(t) = p(t)e^{\zeta t}$ satisfies (7) with $\zeta = \frac{1}{T}\ln\rho(\Phi_{F-V-\varepsilon M}(T)) < 0$ since $\rho(\Phi_{F-V}(T)) < 1$ when $\mathcal{R}_0 < 1$. Consequently, as time t approaches infinity, $Y(t)$ tends to zero, indicating that the zero solution of system (6) is stable on a global scale Thus, as $t \to \infty$, $Y(t) \to 0$, indicating that the zero solution of (6) is globally asymptotically stable. For any $(E(0), C(0), I(0), B(0))^T \in \mathbb{R}^4_+$, we can choose $n^* > 0$ such that $(E(0), C(0), I(0), B(0))^T \leq n^* p(0)$. Using the comparison principle [34] (Theorem B.1), we obtain $(E(t), C(t), I(t), B(t))^T \leq n^* Y(t)$ for all $t > 0$, where $n^* Y(t)$ also satisfies system (7). Consequently, we can deduce that

$$\lim_{t\to\infty}\big(E(t), C(t), I(t), B(t)\big) = (0,0,0,0).$$

By analyzing the derivatives of $S'(t), V'(t)$ in system (1) and considering the behavior of these derivatives as t tends to infinity, we can obtain

$$\begin{aligned}
S^{'}(t) &= \Pi + \theta V(t) - (\xi + \mu)S(t),\\
V'(t) &= \xi S(t) - (\theta + \mu)V(t).
\end{aligned}$$

By the asymptotically periodic semiflow [35] (Theorem 3.2.1) and system (1), we have

$$\lim_{t\to\infty}\big(S(t)-S^*,V(t)-V^*,R(t)\big)=(0,0,0),$$

and the proof is complete. □

3.4. Existence of Positive Periodic Solutions

Theorem 4. *If $\mathcal{R}_0>1$, it can be concluded that the disease is uniformly persistent. Moreover, system (1) possesses at least one positive periodic solution.*

Proof. Define

$$\mathcal{Y}:=\Omega,$$
$$\mathcal{Y}_0:=\{(S,V,E,C,I,R,B)\in\mathcal{Y}:\ E>0,\ C>0,\ I>0,\text{ and } B>0\},$$

and

$$\partial\mathcal{Y}_0:=\mathcal{Y}\setminus\mathcal{Y}_0=\{(S,V,E,C,I,R,B)\in\mathcal{Y}:\ E=0 \text{ or } C=0 \text{ or } I=0 \text{ or } B=0\}.$$

Let $f:\Omega\to\Omega$ be the solution map associated with system (1), and let $f:=f(T)$ represent the Poincaré map corresponding to (1). The expression of f is given by

$$f(u^0)=u(T,u^0),\quad \text{for } u^0\in\mathbb{R}^7_+,$$

where $u(t,u^0)$ denotes the single solution of (1) with initial value $u^0\in\mathcal{Y}$.

Next, we aim to demonstrate that f is uniformly persistent with respect to $(\mathcal{Y}_0,\partial\mathcal{Y}_0)$. Applying [36] (Theorem 3.1.1), we can then conclude that the solution of (1) is uniformly persistent with respect to $(\mathcal{Y}_0,\partial\mathcal{Y}_0)$. Initially, we demonstrate that both $\mathcal{Y}_0$ and $\partial\mathcal{Y}_0$ are positively invariant with respect to system (1). For $\big(S^0,V^0,E^0,C^0,I^0,R^0,B^0\big)\in\mathcal{Y}_0$, solving (1) for all $t>0$, we have

$$S(t)=e^{\int_0^t -a(s)\,ds}\left[S^0+\int_0^t(\Pi+\eta R(s)+\theta V(s))e^{\int_0^s a(r)\,dr}\,ds\right]>0, \tag{9}$$

$$V(t)=e^{\int_0^t -b(s)\,ds}\left[V^0+\int_0^t\xi S(s)e^{\int_0^s b(r)\,dr}\,ds\right]>0, \tag{10}$$

$$E(t)=e^{-(\nu+\mu)t}\left[E^0+\int_0^t\big(S(s)+(1-\alpha)V(s)\big)\big(\lambda_h(s)+\lambda_b(s)\big)e^{(\nu+\mu)s}\,ds\right]>0, \tag{11}$$

$$C(t)=e^{-(\gamma_1+\mu)t}\left[C^0+q\nu\int_0^t E(s)e^{(\gamma_1+\mu)s}\,ds\right]>0, \tag{12}$$

$$I(t)=e^{-(\gamma_2+\mu+\delta)t}\left[I^0+\int_0^t\big((1-q)\nu E(s)+p\gamma_1C(s)\big)e^{(\gamma_2+\mu+\delta)s}\,ds\right]>0, \tag{13}$$

$$R(t)=e^{-(\eta+\mu)t}\left[R^0+\int_0^t\big((1-p)\gamma_1C(s)+\gamma_2I(s)\big)e^{(\eta+\mu)s}\,ds\right]>0, \tag{14}$$

$$B(t)=e^{-\mu_b t}\left[B^0+\int_0^t\big(\tau_1C(s)+\tau_2I(s)\big)e^{\mu_b s}\,ds\right]>0, \tag{15}$$

where $a(t)=\big(\lambda_h(s)+\lambda_b(s)+\xi+\mu\big)$, $b(t)=\big(\lambda_h(t)+\lambda_b(t)+\theta+\mu\big)$. Thus, $\mathcal{Y}_0$ is a positively invariant set. As $\mathcal{Y}$ is also positively invariant and $\partial\mathcal{Y}_0$ is a closed subset contained within $\mathcal{Y}$, it follows that $\partial\mathcal{Y}_0$ is positively invariant.

Given the principle of continuous dependence of the solutions on the initial conditions, we obtain

$$\lim_{u^0\to P^*}\|u(t,u^0)-P^*\|=0,$$

uniformly on $\in [0, T]$. Therefore, for any $\kappa > 0$, there exists a $\sigma = \sigma(\kappa) > 0$, only dependent on κ, such that

$$\|u(t, u^0) - P^*\| < \kappa, \qquad \forall t \in [0, T],$$

whenever $\|u^0 - P^*\| < \sigma$.

Claim 1. $\limsup_{m\to\infty} \|f^m(u^0) - P^*\| \geqslant \sigma$ *for each* $u^0 \in \mathcal{Y}_0$.

By contradiction suppose the claim is not true. Then, there is a $\bar{u}^0 \in \mathcal{Y}_0$ such that

$$\limsup_{m\to\infty} \|f^m(\bar{u}^0) - P^*\| < \sigma,$$

and there exists a $m_0 \in \mathbb{N}$ such that $\|f^m(\bar{u}^0) - P^*\| < \sigma$ for all $m \geq m_0$. Therefore,

$$\|u(t, f^m(\bar{u}^0) - P^*\| < \kappa, \qquad \forall m \geq m_0,\ t \in [0, T].$$

Let $t \geqslant n_0 T$, and we can decompose t as $t = mT + t_1$, where $t_1 \in [0, T)$, and $m = \left[\frac{t}{T}\right]$ denotes the largest integer that does not exceed $\frac{t}{T}$. Then, we obtain

$$\|u\big(t, \bar{u}^0\big) - P^*\| = \|u\big(t_1, f^m(\bar{u}^0)\big) - P^*\| < \kappa, \quad \forall t \geqslant n_0 T,$$

and $S^* - \kappa < S(t) < S^* + \kappa$, $V^* - \kappa < V(t) < V^* + \kappa$, $0 < E(t) < \kappa$, $0 < C(t) < \kappa$, $0 < I(t) < \kappa$, and $0 < B(t) < \kappa$. Then, from system (1), we obtain

$$\begin{aligned}
E^{'}(t) &\geq \big(\lambda_{_h}(t) + \lambda_{_b}(t)\big)\big(S^* - \kappa + (1-\alpha)(V^* - \kappa)\big) - (\nu + \mu)E(t),\\
C^{'}(t) &\geq q\nu E(t) - (\gamma_{_1} + \mu)C(t),\\
I^{'}(t) &\geq (1-q)\nu E(t) + p\gamma_{_1} C(t) - (\gamma_{_2} + \mu + \delta)I(t),\\
B^{'}(t) &\geq \tau_{_1} C(t) + \tau_{_2} I(t) - \mu_b B(t).
\end{aligned}$$

Consider the auxiliary linear system

$$\begin{aligned}
E^{'}(t) &= \big(\lambda_{_h}(t) + \lambda_{_b}(t)\big)\big(S^* - \kappa + (1-\alpha)(V^* - \kappa)\big) - (\nu + \mu)E(t),\\
C^{'}(t) &= q\nu E(t) - (\gamma_{_1} + \mu)C(t),\\
I^{'}(t) &= (1-q)\nu E(t) + p\gamma_{_1} C(t) - (\gamma_{_2} + \mu + \delta)I(t),\\
B^{'}(t) &= \tau_{_1} C(t) + \tau_{_2} I(t) - \mu_b B(t).
\end{aligned} \tag{16}$$

Since $\mathcal{R}_0 > 1$, we know from Theorem 1 that $\rho(\Phi_{F-V}(T)) > 1$. Therefore, it is possible to choose $\kappa > 0$ small enough so that we have $\rho(\Phi_{F-V-\kappa M}(T)) > 1$, where $M(t)$ is defined in (8). By [33] (Lemma 2.1) it is possible to find a positive function $q(t)$ with a period of T such that $g(t) = (E(t), C(t), I(t), B(t)) = q(t)e^{\chi t}$ is a solution of (16) and $\chi = \frac{1}{T}\ln\rho(\Phi_{F-V-\kappa M}(T)) > 0$. As $\mathcal{R}_0 > 1$ and $\rho(\Phi_{F-V-\kappa M}(T)) > 1$, if $g(0) > 0$, $g(t) \to \infty$ as $t \to \infty$. Utilizing the comparison principle [34] (Theorem B.1), we obtain $E(0) > 0$, $C(0) > 0$, $I(0) > 0$, $B(0) > 0$, $\lim_{t\to\infty} E(t) = \infty$, $\lim_{t\to\infty} C(t) = \infty$, $\lim_{t\to\infty} I(t) = \infty$, and $\lim_{t\to\infty} B(t) = \infty$. This statement contradicts conditions $E(t) < \kappa$, $C(t) < \kappa$, $I(t) < \kappa$, $B(t) < \kappa$. Therefore, this claim is valid.

Let us introduce

$$M_\partial = \Big\{u^0 \in \partial\mathcal{Y}_0 : f^m(u^0) \in \partial\mathcal{Y}_0,\ \forall m \in \mathbb{N}\Big\}.$$

Claim 2. $M_\partial = \big\{\big(S(0), V(0), E(0), C(0), I(0), R(0), B(0)\big) :\ S > 0, V > 0\big\}$.

Let us note that $M_\partial \supseteq \{(S(0), V(0), E(0), C(0), I(0), R(0), B(0)) : S > 0, V > 0\}$. It suffices to prove that $M_\partial \subset \{(S, V, 0, 0, 0, 0, 0) : S > 0, V > 0\}$ for arbitrary initial condition $u^0 \in \partial\mathcal{Y}_0$, $E(nT) = 0$, $C(nT) = 0$, $I(nT) = 0$, or $B(nT) = 0$, for all $n \geqslant 0$.

Let us consider a scenario where, for the purpose of contradiction, there exists an integer $n_1 \geqslant 0$ such that $E(n_1T) > 0$, $C(n_1T) > 0$, $I(n_1T) = 0$, and $B(n_1T) = 0$. Then, placing $t = n_1T$ in place of the initial time $t = 0$ in (9)–(15), we obtain $S(t) > 0$, $V(t) > 0$, $E(t) > 0$, $C(t) > 0$, $I(t) > 0$, $R(t) > 0$, and $B(t) > 0$. This contradicts the positive invariance of $\partial\mathcal{Y}_0$. This provides proof for Claim 2 stated earlier.

Claim 1 implies that f is weakly uniformly persistent with respect to $(\mathcal{Y}_0, \partial\mathcal{Y}_0)$. Proposition 1 ensures the existence of a global attractor of f. Consequently, P^* represents an isolated invariant set in $\mathcal{Y}$ and $W^s(P^*) \cap \mathcal{Y}_0 = \emptyset$. By Claim 2, each solution in M_∂ tends to P^*, and P^* is clearly acyclic in M_∂. By [36] (Theorem 1.3.1 and Remark 1.3.1), we can deduce that f is uniformly (strongly) persistent with respect to $(\mathcal{Y}_0, \partial\mathcal{Y}_0)$. Therefore, there is an $\varepsilon > 0$ such that $\liminf_{t\to\infty} (E(t), C(t), I(t), R(t), B(t)) \geqslant (\varepsilon, \varepsilon, \varepsilon, \varepsilon, \varepsilon)$, for all $u^0 \in \mathcal{Y}_0$. By [35] (Theorem 1.3.10), f has a fixed point $\bar{\phi} \in \mathcal{Y}_0$, and therefore system (1) has at least one periodic solution $u(t, \bar{\phi})$ with $\bar{\phi} = (\bar{S}(0), \bar{V}(0), \bar{E}(0), \bar{C}(0), \bar{I}(0), \bar{R}(0), \bar{B}(0)) \in \mathcal{Y}_0$. We now demonstrate that $\bar{S}(0)$ is positive. Suppose that $\bar{S}(0) = 0$, then we obtain $\bar{S}(0) > 0$ for all $t > 0$. However, considering the periodicity of the solution, we find $\bar{S}(0) = \bar{S}(nT) = 0$, which leads to a contradiction. □

4. Model Calibration, Sensitivity Analysis, and Prediction

Based on the work by [29], we make the assumption that the time-varying transmission rate, denoted as $\beta_b(t)$, follows the equation: Here, $\tilde{\beta}_b$ represents the baseline long-cycle transmission rate, Λ represents the amplitude of seasonal forcing, and φ represents the seasonal offset parameter.

4.1. Model Fitting to Typhoid Fever Data from Taiwan

According to the source cited [37], the average population in Taiwan in 2023 was reported to be 23,257,434 with a corresponding life expectancy of 80.09 years. Consequently, the human death rate (μ) can be calculated per day and its inverse (μ^{-1}) can be determined as 80.09×365. Subsequently, the recruitment rate of humans (Π) can be obtained by multiplying 23,257,434 by μ, resulting in a value of 795.592. Our study used model (1) to fit the cumulative number of annual cases and newly infected cases per year of the documented outbreak of typhoid fever in Taiwan that ranged from 2008 to 2023. Time series data for cases of typhoid fever were obtained from the Taiwan National Infectious Diseases Statistics System [38]. To estimate the parameters of the typhoid fever model, we utilized Latin hypercube sampling and least squares techniques [39], which provided us with parameter estimates for the typhoid model (1).

Figure 2 illustrates the fit of the model with the typhoid fever data from Taiwan, demonstrating a satisfactory agreement between the model and the observed cumulative cases of infection (left panel) as well as newly infected cases (right panel). This indicates that the model effectively captures the essential patterns of incidence of typhoid fever between 2008 and 2023. The parameter values, ranges, and units that yield the best fit in Figure 2 are presented in Table 2. Using these parameter values and the methodology established in Mitchell and Kribs [40], we numerically estimated Taiwan's current basic reproduction number, $\mathcal{R}_0$, to be approximately 0.995393. This value suggests that the disease is expected to fade away within the population as $\mathcal{R}_0 < 1$, indicating that transmission is not sustainable in the long term.

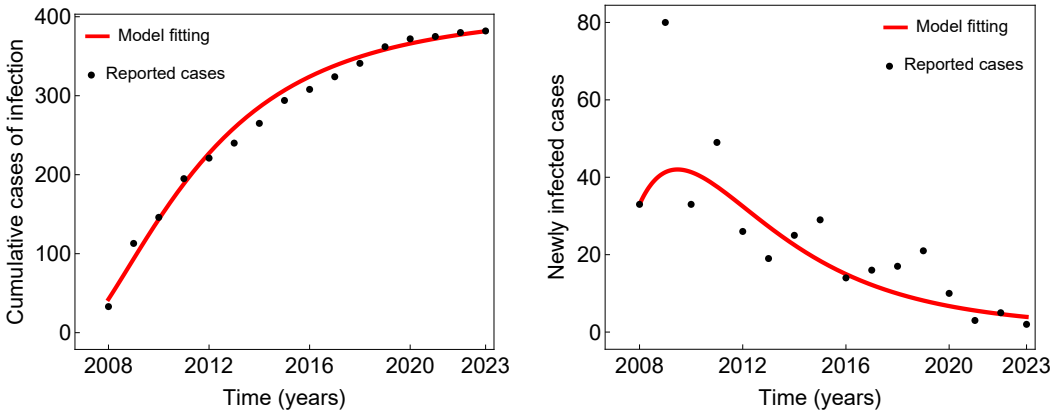

Figure 2. Fitting model results for cumulative infected cases (**left**) and newly infected cases (**right**) in Taiwan from 2009 to 2023. The fitting was based on the parameter values provided in Table 2 and the initial conditions were set as $S^0 = 2000$, $V^0 = 20$, $E^0 = 100$, $I^0 = 33$, $C^0 = 20$, $R^0 = 5$, and $B^0 = 2000$.

Table 2. Parameters values, ranges, and units for model (1).

Parameters	Baseline Values	Range	Units	Source
Π	795.592	-	Persons per day	[37]
μ	3.42081×10^{-5}	-	Per day	[37]
β_1	10^{-8}, 10^{-8}	0–0.1	Per day	[22,29]
β_2	10^{-8}, 10^{-8}	0–0.1	Per day	[22,29]
τ_1, τ_2	0.81, 0.75	0–1	Per day	[24,29]
$\tilde{\beta}_b$	10^{-9}	0–0.1	Per day	[24,29]
Λ	0.797	0–1	-	[24,29]
φ	4.37	1–10	-	[24,29]
p	0.5	0–1	Per day	[22,27]
q	0.1	0–1	Per day	[22,27]
γ_1, γ_2	0.127, 0.357	0–1	Per day	[22,27]
ν	0.378	0–1	Per day	[41,42]
δ	0.079	0–0.5	Per day	[41]
α	0.75	0.5–0.956	Per day	[27,30]
η, θ	0.054, 0.0292	0.00833–0.6	Per day	[41,43]
ξ	0.054	0.05–0.5	Per day	[27,29]
μ_b	0.217	0.001–0.5	Per day	[29,44]

4.2. Sensitivity Analysis

Sensitivity analysis is a method used to assess how uncertainty in a model's parameters contributes to the overall uncertainty in its predictions [45]. By identifying influential parameters and evaluating their impact on output variability, sensitivity analysis helps us understand the relationships between the system's parameters and its outcomes.

An approach commonly used in sensitivity analysis is the calculation of sensitivity indices [46]. These indices quantify the proportional impact of parameter variations on a specific output or state variable. In particular, the normalized forward sensitivity index is used when analyzing the influence of differentiable variables (x) with respect to a parameter (p). It compares the relative changes in x and p and can be mathematically expressed as

$$\Psi_p^x = \frac{\partial x}{\partial p} \times \frac{p}{x}.$$

To determine the basic reproduction number $\mathcal{R}_0^A$ for the autonomous version of the model (1), we relied on the findings of the study conducted by [47]. In this scenario, we assumed that $\beta_b(t)$ was a constant $\bar{\beta}_b$ for all $t \geq 0$. This allowed us to apply the results of the aforementioned study to estimate $\mathcal{R}_0^A$ as follows

$$\begin{aligned}\mathcal{R}_0^A =&(S^* + (1-\alpha)V^*)\left[\frac{q\beta_1\nu}{(\gamma_1+\mu)(\mu+\nu)} + \frac{\beta_2\nu(p\gamma_1 q + (1-q)(\gamma_1+\mu))}{(\gamma_1+\mu)(\gamma_2+\delta+\mu)(\mu+\nu)}\right.\\ &\left.+\nu\bar{\beta}_b\left(\frac{q\tau_1}{\mu_b(\gamma_1+\mu)(\mu+\nu)} + \frac{\tau_2(p\gamma_1 q + (1-q)(\gamma_1+\mu))}{\mu_b(\gamma_1+\mu)(\gamma_2+\delta+\mu)(\mu+\nu)}\right)\right].\end{aligned} \tag{17}$$

To assess the sensitivity of $\mathcal{R}_0^A$ given by (17), a sensitivity analysis was performed. Specific parameter values were selected for the analysis, which is presented in Table 2. The sensitivity indices for $\mathcal{R}_0^A$ are provided in Table 3. According to the data provided in Table 3, reducing the values of parameters such as β_2, $\bar{\beta}_b$, τ_2, q, β_1, θ, τ_1, and p by 10% results in an approximate decrease in $\mathcal{R}_0^A$ by approximately 4.49%, 3.88%, 2.79%, 2.32%, 1.62%, 1.1%, 1.08%, and 0.383%, respectively. On the other hand, increasing the values of parameters such as μ, γ_2, μ_b, γ_1, α, δ, and ξ by 10% leads to an approximate decrease in $\mathcal{R}_0^A$ by 9%, 5.96%, 3.88%, 2.71%, 1.32%, 1.32%, and 1.17%, respectively.

Table 3. Sensitivity indices of $\mathcal{R}_0^A$ to parameters in model (1), assessed by employing the baseline parameter values provided in Table 2.

Parameter	μ	γ_2	β_2	$\bar{\beta}_b$	μ_b	τ_2
Sensitivity index	−0.901	−0.596	0.449	0.388	−0.388	0.279
Parameter	γ_1	q	β_1	α	δ	ξ
Sensitivity index	−0.271	0.232	0.162	−0.132	−0.132	−0.117
Parameter	θ	τ_1	p	ν		
Sensitivity index	0.1116	0.1089	0.0383	0.000087		

The results shown in Figure 3 indicate that the basic reproduction number $\mathcal{R}_0^A$ is highly sensitive to several parameters. The most influential factors that impact $\mathcal{R}_0^A$ include the natural mortality rate (μ), recovery rates (γ_1 and γ_2), human-to-human infection rates (β_1 and β_2), bacterial decay rate (μ_b), and relative infectiousness (τ_2 and τ_1). Additionally, vaccine efficiency (α), vaccine coverage (ξ), and disease-induced mortality (δ) also exhibit significant sensitivity in relation to $\mathcal{R}_0^A$. These findings highlight the importance of accurately estimating and considering these parameters in analyzing the transmission dynamics and control measures of the disease.

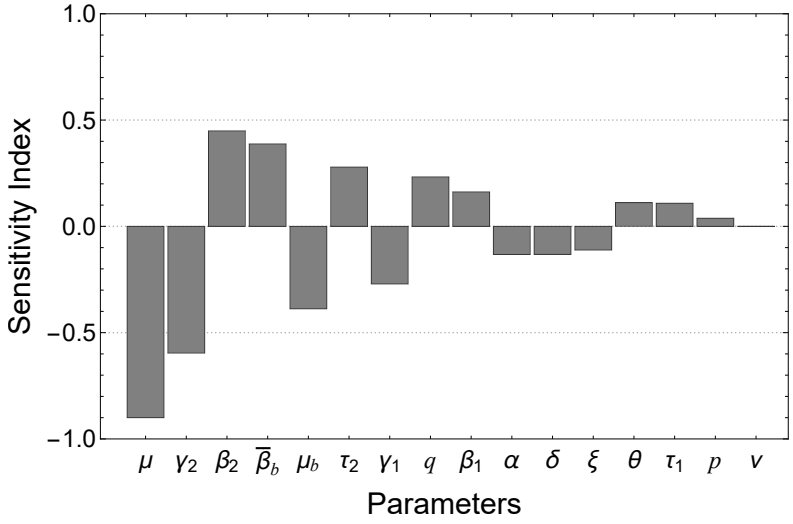

Figure 3. Sensitivity analysis for $\mathcal{R}_0^A$, using the parameter values specified in Table 2. Sensitivity indices are presented in descending order of magnitude.

4.3. Prediction of New Typhoid Infections in Taiwan

Based on the findings presented in Figure 4, it can be concluded that the estimated number of newly infected cases will gradually approach zero over the course of a few years. As a result, the cumulative number of new typhoid cases will reach a steady state (approximately 400 cases) and will remain constant.

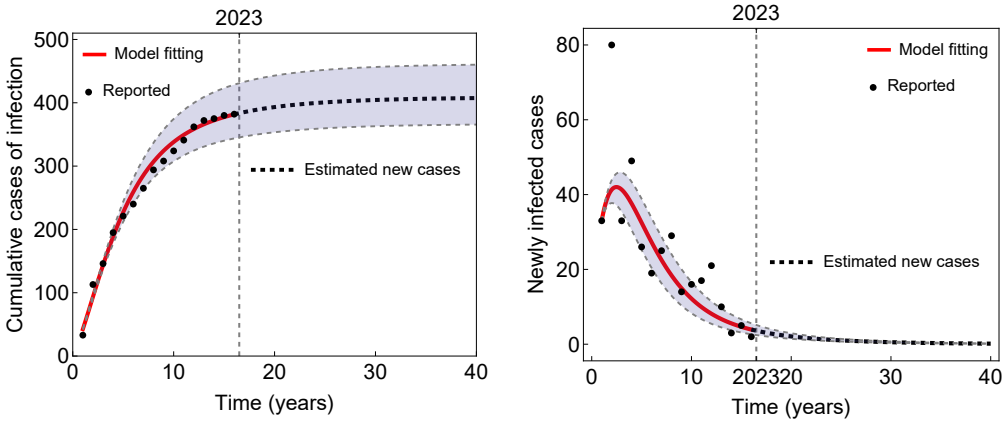

Figure 4. Prediction of new typhoid infections in Taiwan with the parameter values provided in Table 2.

One of the primary objectives of this study was to investigate the potential parameter changes that could contribute to an increase in the number of infected cases and potentially lead to a future typhoid epidemic in Taiwan over the next few years. Due to the extensive number of parameters involved, conducting a rigorous assessment to determine the most influential parameters in the variation of the dynamics is challenging. Therefore, in this study, we focused on demonstrating potential alterations through three specific examples as shown in Figure 5.

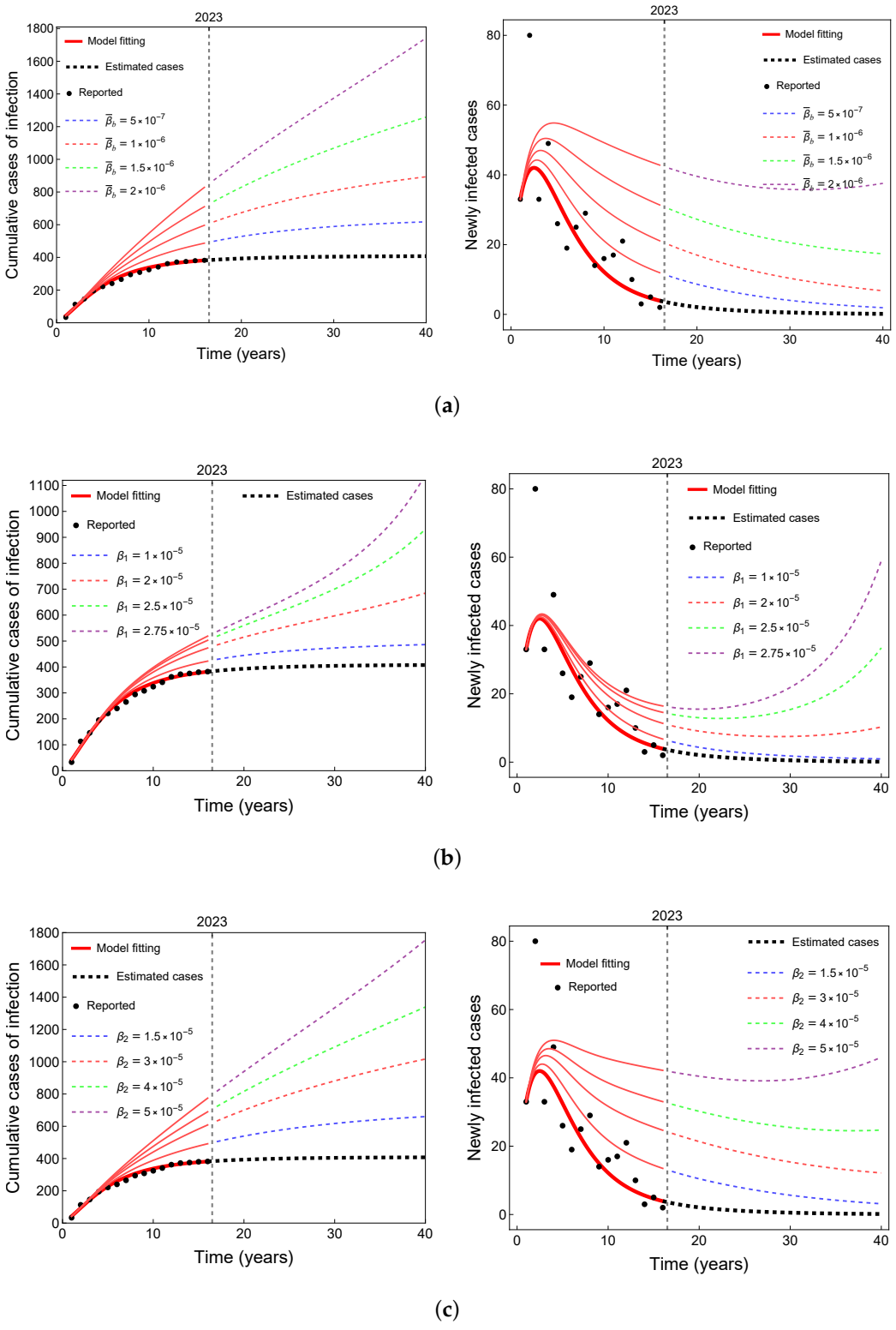

Figure 5. Prediction of new typhoid infections with respect to (**a**) $\bar{\beta}_b$, (**b**) β_1, and (**c**) β_2 in Taiwan and the rest of the parameter values provided in Table 2.

In Figure 5, we provide an estimate of the possible impact of changes in key parameters, including human-to-human transmission rates (β_1 and β_2) and bacteria-to-human transmission rate ($\bar{\beta}_b$), on the progression of typhoid epidemics in Taiwan. The simulations carried out reveal that an increase in any of these three parameters, whether through direct transmission (see Figure 5b,c) or indirect transmission (see Figure 5a), can result in a sub-

stantial increase in the number of typhoid infections. Moreover, such parameter changes can lead to the emergence of periodic annual epidemics, characterized by the reappearance of typhoid cases on a recurring basis. These findings underscore the importance of closely monitoring and effectively managing these parameters to prevent and control possible outbreaks of typhoid in Taiwan.

5. Numerical Simulations

In this section, we present numerical simulations aimed at illustrating and validating the theoretical findings discussed earlier. These simulations serve as visual evidence to demonstrate the agreement between our time-periodic model and the observed seasonal fluctuations.

5.1. Extinction and Persistence

The significance of the basic reproduction number ($\mathcal{R}_0$) as a threshold parameter for determining the persistence or extinction of the disease within the population is highlighted in Section 3. The numerical results presented in Figures 6 and 7 provide compelling evidence that the solutions obtained from our model (1) are consistent with the analytical findings. These results demonstrate that the disease-free periodic solution P^* maintains a global asymptotic stability when condition $\mathcal{R}_0 \approx 0.995393 < 1$ is satisfied, leading to disease extinction within the population.

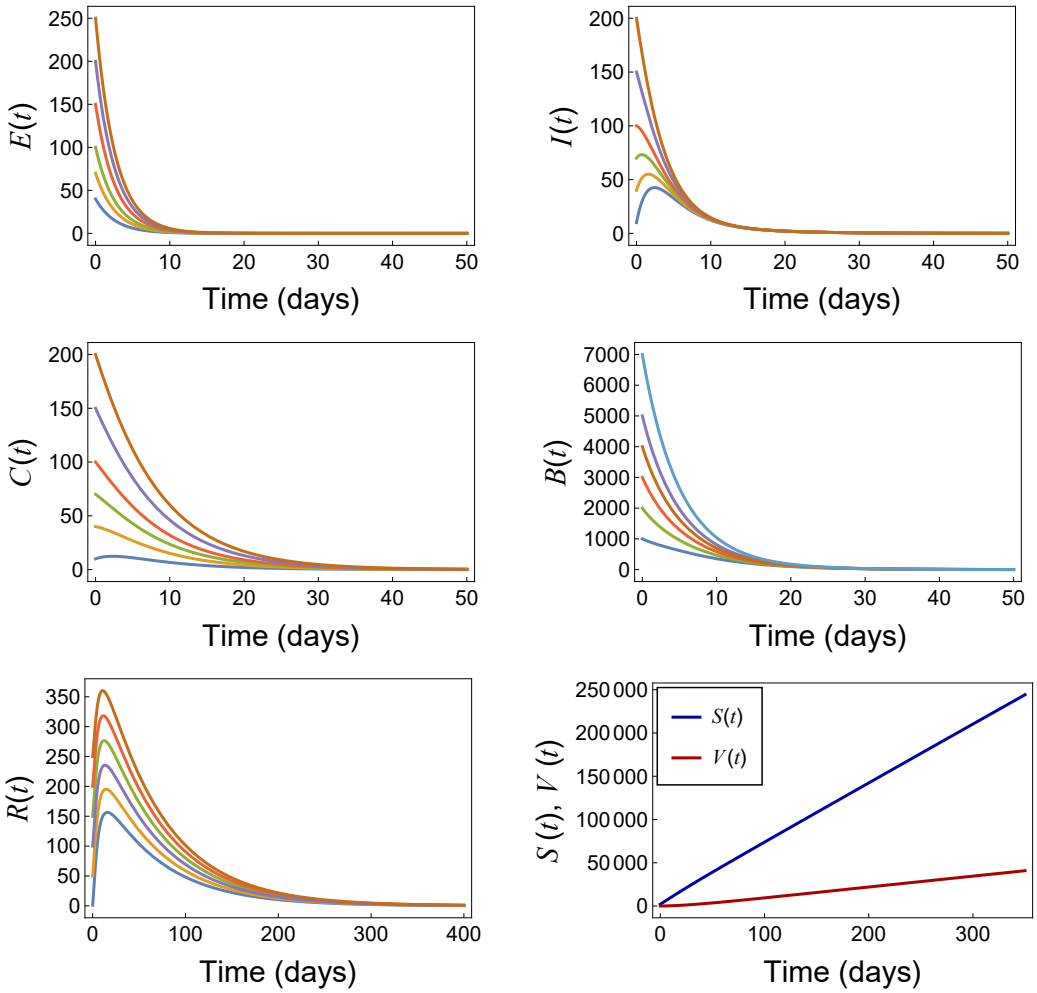

Figure 6. Extinction of the disease with the parameter values provided in Table 2 when $\mathcal{R}_0 \approx 0.995393 < 1$.

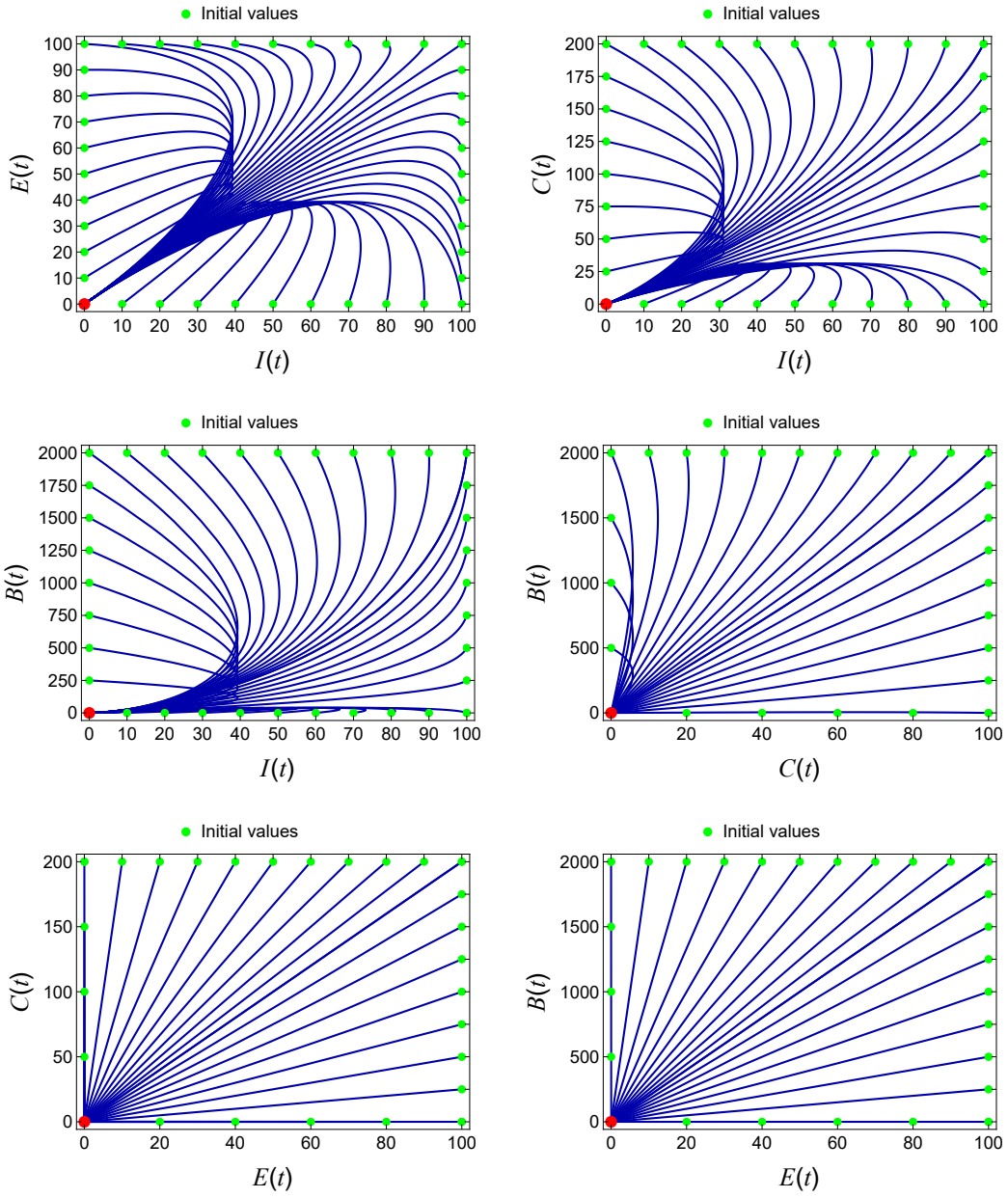

Figure 7. Global stability of P^* with the parameter values provided in Table 2 when $\mathcal{R}_0 \approx 0.995393 < 1$.

To demonstrate the persistence of the disease, we conducted simulations using various parameter sets. Here, we present two examples showing how the disease persists with a high number of infections due to the elevated value of $\mathcal{R}_0$.

Example 1. *Figure 8 displays the simulation results using the parameter set given in Table 4. With a* $\mathcal{R}_0 \approx 2.04735$ *value exceeding the threshold of 1, the disease exhibits persistent dynamics. The graph illustrates a high number of infections sustained over time, indicating the continued transmission and presence of the disease within the population.*

Example 2. *Figure 9 presents the simulation results using the parameter set given in Table 5. Similarly, the elevated value* $\mathcal{R}_0 \approx 14.8345$ *leads to the persistence of the disease, as depicted by the high sustained number of infections shown in the graph. This example further illustrates the continued transmission and enduring presence of the disease within the population.*

By running simulations with different parameter sets, these examples provide clear evidence of the persistence of the disease, highlighting the direct correlation between the high $\mathcal{R}_0$ value and the sustained number of infections and confirming the existence of a positive periodic solution, as shown in Figure 10.

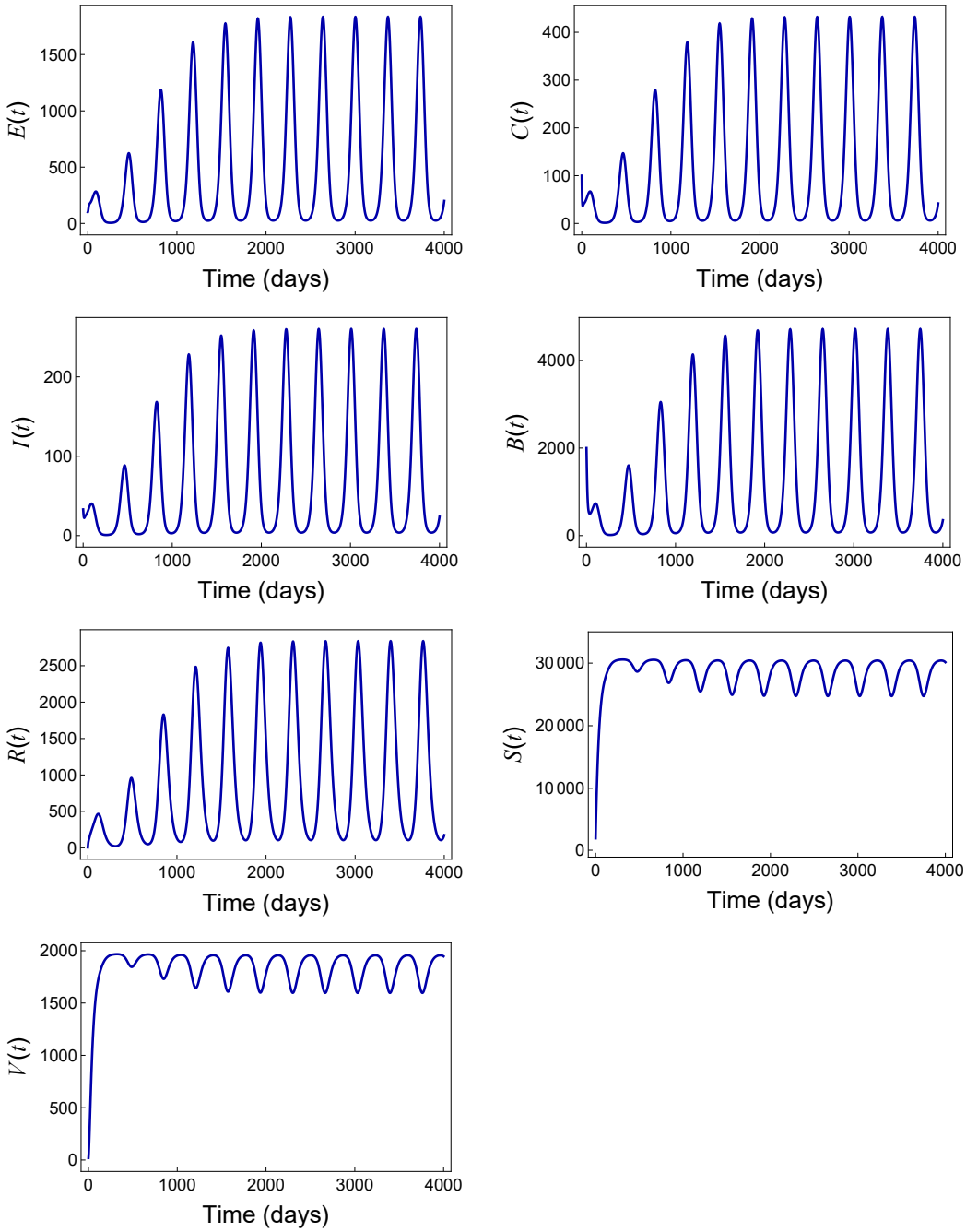

Figure 8. Persistence of the disease with the parameter values provided in Table 4 when $\mathcal{R}_0 \approx 2.04735 > 1$.

Table 4. Parameters and values for model (1) (persistence Example 1).

Parameters	Π	μ	β_1	β_2	τ_1	τ_2	$\bar{\beta}_b$
Values	795.592	0.0235	10^{-6}	10^{-6}	0.81	0.75	1.4×10^{-6}
Parameters	Λ	φ	p	q	γ_1	γ_2	ν
Values	0.763	2.88	0.152	0.7402	0.233	0.04	0.082
Parameters	δ	α	η	ξ	θ	μ_b	$\mathcal{R}_0$
Values	0.144	0.95	0.0043	0.0054	0.0604	0.111	2.04735

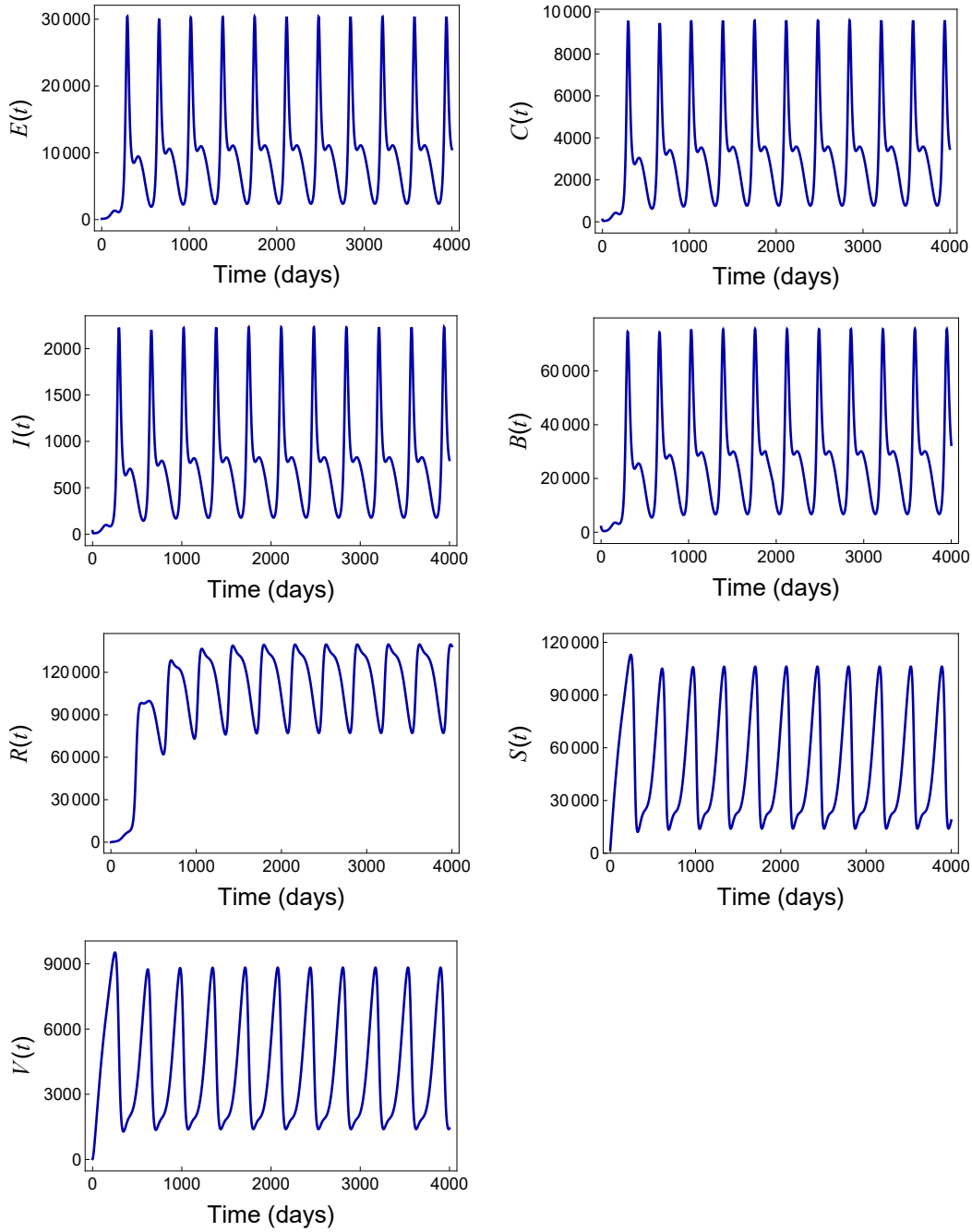

Figure 9. Persistence of the disease with the parameter values provided in Table 5 when $\mathcal{R}_0 \approx 14.8345 > 1$.

Table 5. Parameters and values for model (1) (persistence Example 2).

Parameters	Π	μ	β_1	β_2	τ_1	τ_2	$\bar{\beta}_b$
Values	795.592	0.00235	10^{-6}	10^{-6}	0.81	0.75	10^{-6}
Parameters	Λ	φ	p	q	γ_1	γ_2	ν
Values	0.763	2.88	0.312	0.702	0.233	0.304	0.1082
Parameters	δ	α	η	ξ	θ	μ_b	$\mathcal{R}_0$
Values	0.44	0.95	0.0043	0.0054	0.0604	0.111	14.8345

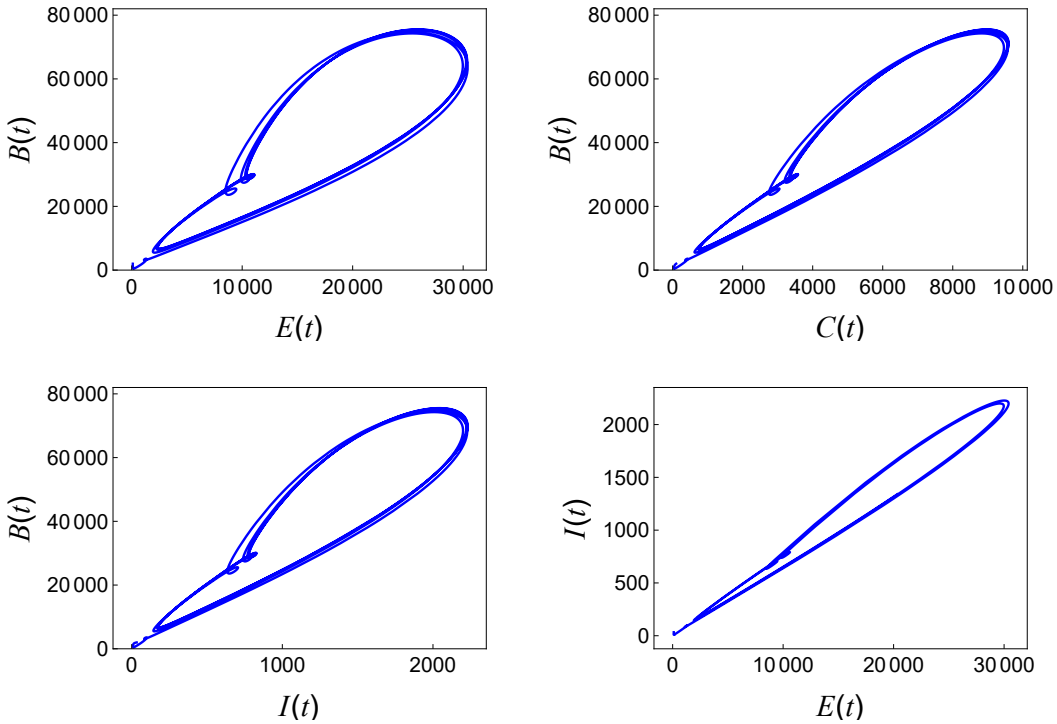

Figure 10. Positive periodic solutions with the parameter values provided in Table 5 when $\mathcal{R}_0 \approx 14.8345 > 1$.

5.2. Vaccine Coverage and Efficiency

As demonstrated in Figure 11a, it becomes evident that an increase in the vaccination coverage rate (ξ) leads to a significant reduction in the number of typhoid cases. Achieving this result poses a challenge in developing countries of South Asia such as India, Pakistan, and Bangladesh. Although the specific situation in Taiwan is unknown to us, it appears that Taiwan demonstrates the feasibility of high vaccination coverage, considering the relatively low number of typhoid infections. To tackle this problem, it is imperative that the government implements a highly effective vaccine (α), as illustrated in Figure 11b. Simultaneously, it is essential to ensure the accessibility of the vaccine, particularly for people living in poverty.

In our model, similar to other compartment models that consider imperfect vaccines, we made the assumption that the immunity acquired through vaccination is temporary. This means that vaccinated individuals can experience a decrease in immunity over time, leading to a possible loss of protection against the disease. This assumption is supported by Figure 11c, which shows that the rate at which vaccinated individuals lose their immunity (θ) also has an impact on the infectious population. A higher value of θ indicates a faster loss of immunity, leading to an increase in the number of infected individuals over time.

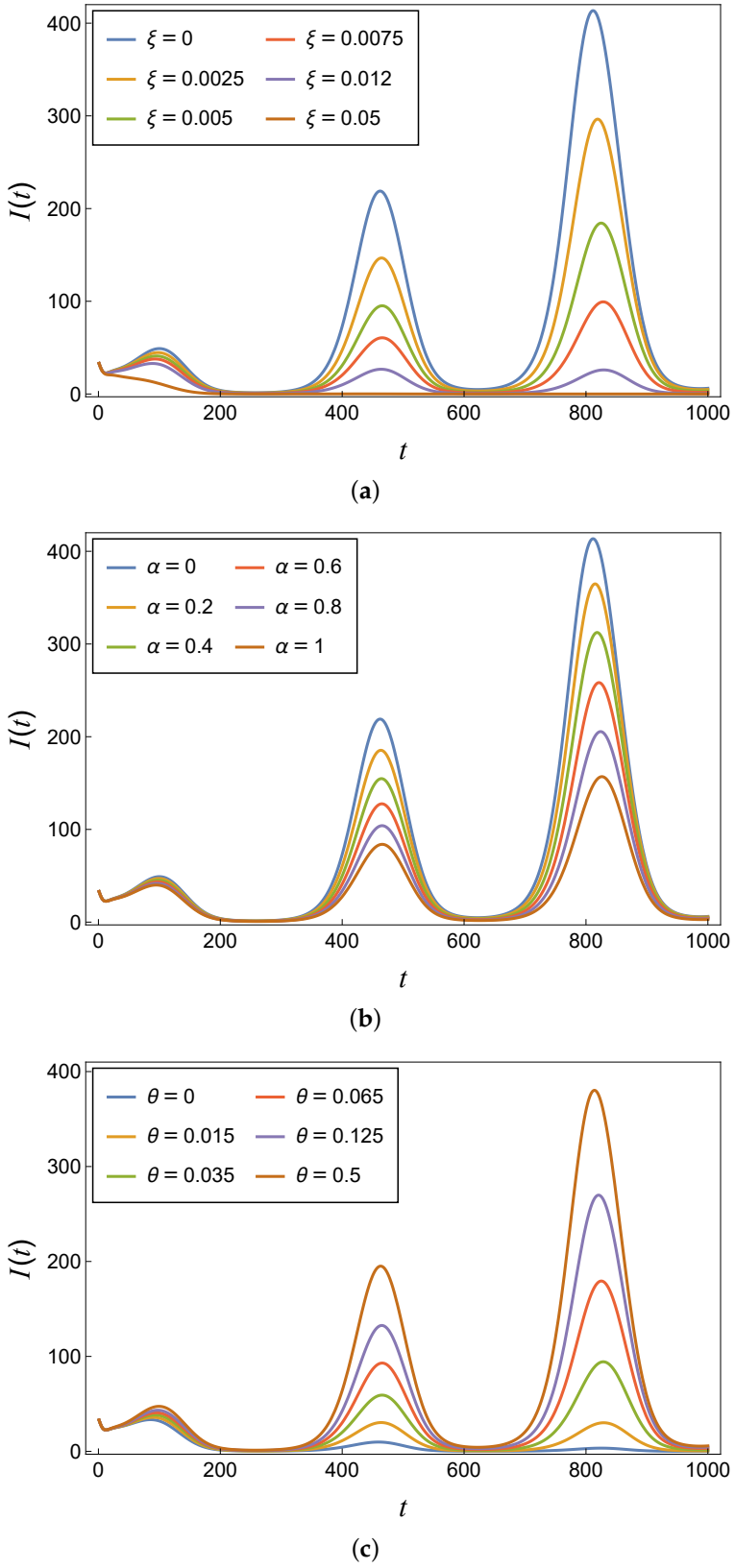

Figure 11. Infectious population under varying values of (**a**) vaccine coverage rate (ξ), (**b**) vaccine efficacy (α), and (**c**) vaccinated losing immunity rate (θ), using the parameter values provided in Table 4.

It is important to note that a low efficacy rate (α) is comparatively less problematic than a low vaccine coverage rate (ξ), as indicated in Figure 11. A higher vaccine coverage rate plays a crucial role in suppressing the epidemic and thus underscores its significance in alleviating the burden associated with this disease. Ideally, the administration of the typhoid vaccine should occur at least one month prior to travel. However, if circumstances require it, the vaccine can be administered closer to the travel date. In the United States, routine typhoid vaccination is not recommended. However, if there is an ongoing risk of bacterial infection by typhoid, it is recommended to receive booster vaccinations every three years, as recommended by the CDC [48].

6. Discussion and Conclusions

We developed a nonautonomous compartmental model that described the transmission of typhoid fever in a seasonal environment. This model incorporated vaccination and accounted for the periodic indirect transmission of the disease. The behavior of the system described by Equation (1) was influenced by the basic reproduction number, $\mathcal{R}_0$. If $\mathcal{R}_0 < 1$, the disease-free solution was globally asymptotically stable, indicating the successful elimination of typhoid fever within the population. In contrast, if $\mathcal{R}_0 > 1$, we showed that there was at least one periodic solution, which confirmed the persistence of typhoid fever within the population. To validate these theoretical findings, numerical simulations were conducted, and their results shown in Figures 6–10.

To accurately fit the cumulative number of annual and newly infected cases during the reported typhoid fever outbreak in Taiwan from 2008 to 2023, we applied model (1) in our study. Parameter estimation was performed using Latin hypercube sampling and least squares techniques. Through a numerical analysis, we discovered that the current basic reproduction number in Taiwan was below the threshold of one, implying the successful elimination of typhoid fever within the population. Furthermore, we conducted a sensitivity analysis to assess the impact of various parameters on the basic reproduction number $\mathcal{R}_0^A$ of the autonomous version of the model (1). The findings indicated that $\mathcal{R}_0^A$ was significantly influenced by several factors, including the natural mortality rate (μ), recovery rates (γ_1 and γ_2), human-to-human infection rates (β_1 and β_2), bacterial decay rate (μ_b), and relative infectiousness (τ_2 and τ_1). This analysis provided crucial information on the key determinants that affect the potential spread and control of typhoid fever within the population. Our investigation of the possible changes in parameters that affect typhoid cases and the likelihood of a future epidemic in Taiwan revealed important information. By examining key parameters such as human-to-human transmission rates (β_1 and β_2) and the bacteria-to-human transmission rate ($\bar{\beta}_b$), we evaluated their impact on the progression of typhoid epidemics. The findings, as depicted in Figure 5, indicated that variations in these parameters could lead to the occurrence of recurring annual epidemics, with typhoid cases periodically reappearing. This underscores the need for vigilant monitoring and effective management of these parameters to mitigate the risk of possible typhoid outbreaks in Taiwan. By closely understanding the factors driving the transmission of typhoid, appropriate measures can be implemented to prevent and control future epidemics in the region.

Our findings indicated that increasing the rate of vaccination coverage (ξ) had a positive effect on reducing the number of typhoid cases, as evidenced in Figure 11a. This poses a significant challenge for developing countries in South Asia. To address this problem, it becomes crucial to introduce a highly effective vaccine (α), as illustrated in Figure 11b, and ensure its accessibility to individuals in impoverished communities. This emphasizes the critical role of achieving a higher vaccination coverage rate (ξ) in suppressing the epidemic and alleviating its associated burden, surpassing the implications of a low efficacy rate (α).

Karunditu et al. [12] established a model to study the transmission of typhoid fever, focusing on human-to-human transmission. In our study, we built and studied a nonautonomous model that considered vaccination and addressed both direct and indirect (periodic) transmission of the disease. Furthermore, our model was based on autonomous

models explored by the authors in [21,27] incorporating temporal periodicity, vaccination, and accounting for seasonal fluctuations in transmission rates correlated with rainfall patterns. Unlike the work of Irena and Gakkhar [49], who focused on the coinfection dynamics of HIV and typhoid, our study explored a distinct aspect of the dynamics of typhoid fever without addressing coinfections. Furthermore, our model differed from that constructed by Musa et al. [22], which examined the effectiveness of public health education programs. Instead, our focus was on developing and analyzing a periodic model that incorporated vaccination and accounted for the periodic indirect transmission of the disease, as well as predicting future epidemics in Taiwan. Although Syed et al. [30] provides an overview of licensed typhoid vaccines and vaccine candidates, our main focus lay in developing and analyzing our nonautonomous system in a seasonal environment, specifically studying the impact of coverage and efficacy of vaccination on suppressing future typhoid epidemics. The study by [26] found that increasing interaction rates between susceptible and infected populations led to higher basic reproduction numbers, indicating increased disease spread. Controlling transmission could be achieved by reducing interaction rates.

In general, our study confirmed that our periodic model effectively captured seasonal variations in disease transmission. We calibrated the model using real data from Taiwan and identified key parameters that contributed to disease spread through a sensitivity analysis. Specifically, we evaluated the impact of imperfect vaccination and generated predictions for new typhoid cases. To validate our findings, we conducted numerical simulations. However, the present study offers insights and applications to help public health departments combat typhoid fever transmission:

- **Identifying key parameters:** Through a sensitivity analysis, our study identified crucial factors that influence typhoid spread. Public health departments can prioritize interventions and allocate resources accordingly. Taking steps to reduce human-to-human transmission rates and improve hygiene and sanitation practices helps control transmission.
- **Predicting future epidemics:** Our periodic model and simulations allow the prediction of future typhoid epidemics. Public health departments can anticipate and prepare for outbreaks by implementing preventive measures such as a better surveillance, public awareness campaigns, and improved response strategies.
- **Vaccination:** The study emphasized the importance of vaccination in reducing cases of typhoid. Public health departments can use this information to develop targeted vaccination campaigns, focusing on areas with low coverage. Increasing vaccination rates and ensuring access to effective vaccines can mitigate the risk of typhoid outbreaks.

In summary, to mitigate the risk of typhoid fever outbreaks and improve public health, it is crucial to strengthen vaccination efforts by increasing coverage rates and ensuring access to effective vaccines. For optimal protection, the typhoid vaccine should ideally be administered at least one month before travel, but it can be administered closer to the travel date if necessary. Routine vaccination against typhoid is not recommended in the US, for example, but booster vaccinations are recommended every three years for those at ongoing risk by the CDC [48]. Furthermore, continuous monitoring of transmission parameters, improving surveillance systems, promoting hygiene and sanitation practices, enhancing public awareness, and fostering collaboration among stakeholders are essential steps. By implementing these measures, we can proactively prevent and control outbreaks of typhoid fever, safeguarding the health and well-being of communities at risk.

Author Contributions: Conceptualization, M.H.A., F.K.A. and M.A.I.; methodology, M.H.A., F.K.A. and M.A.I.; software, M.H.A., F.K.A. and M.A.I.; validation, M.H.A., F.K.A. and M.A.I.; formal analysis, M.A.I.; investigation, M.H.A., F.K.A. and M.A.I.; writing—original draft preparation, M.H.A., F.K.A. and M.A.I.; writing—review and editing, M.H.A., F.K.A. and M.A.I.; visualization, M.H.A., F.K.A. and M.A.I.; funding acquisition, M.H.A. All authors have read and agreed to the published version of the manuscript.

Funding: This work was funded by the University of Jeddah, Jeddah, Saudi Arabia, under grant No. (UJ-23-DR-4).

Data Availability Statement: Not applicable.

Acknowledgments: This work was funded by the University of Jeddah, Jeddah, Saudi Arabia, under grant No. (UJ-23-DR-4). The authors, therefore, thank the University of Jeddah for its technical and financial support.

Conflicts of Interest: The authors declare no conflict of interest.

References

1. James, S.L.; Abate, D.; Abate, K.H.; Abay, S.M.; Abbafati, C.; Abbasi, N.; Abbastabar, H.; Abd-Allah, F.; Abdela, J.; Abdelalim, A.; et al. Global, regional, and national incidence, prevalence, and years lived with disability for 354 diseases and injuries for 195 countries and territories, 1990–2017: A systematic analysis for the Global Burden of Disease Study 2017. *Lancet* **2018**, *392*, 1789–1858.
2. Crump, J.A.; Sjölund-Karlsson, M.; Gordon, M.A.; Parry, C.M. Epidemiology, clinical presentation, laboratory diagnosis, antimicrobial resistance, and antimicrobial management of invasive Salmonella infections. *Clin. Microbiol. Rev.* **2015**, *28*, 901–937. [CrossRef] [PubMed]
3. Centers for Disease Control and Prevention. Typhoid Fever and Paratyphoid Fever. Available online: https://www.cdc.gov/typhoid-fever/index.html (accessed on 1 June 2023).
4. World Health Organization. Typhoid. Available online: https://www.who.int/news-room/fact-sheets/detail/typhoid (accessed on 1 June 2023).
5. Mogasale, V.; Maskery, B.; Ochiai, R.L.; Lee, J.S.; Mogasale, V.V.; Ramani, E.; Kim, Y.E.; Park, J.K.; Wierzba, T.F. Burden of typhoid fever in low-income and middle-income countries: A systematic, literature-based update with risk-factor adjustment. *Lancet Glob. Health* **2014**, *2*, e570–e580. [CrossRef] [PubMed]
6. Bhutta, Z.A. Current concepts in the diagnosis and treatment of typhoid fever. *BMJ* **2006**, *333*, 78–82. [CrossRef]
7. Ackers, M.L.; Puhr, N.D.; Tauxe, R.V.; Mintz, E.D. Laboratory-based surveillance of Salmonella serotype Typhi infections in the United States: Antimicrobial resistance on the rise. *JAMA* **2000**, *283*, 2668–2673. [CrossRef]
8. Mirza, S.; Beechmg, N.; Hart, C. Multi-drug resistant typhoid: A global problem. *J. Med Microbiol.* **1996**, *44*, 317–319. [CrossRef]
9. L'Organisation mondiale de la Santé, O.; World Health Organization. Typhoid vaccines: WHO position paper–March 2018–Vaccins antityphoïdiques: Note de synthèse de l'OMS–mars 2018. *Wkly. Epidemiol. Rec. = Relevé Épidémiologique Hebd.* **2018**, *93*, 153–172.
10. Mushayabasa, S. A simple epidemiological model for typhoid with saturated incidence rate and treatment effect. *Int. J. Math. Comput. Sci.* **2013**, *6*, 688–695.
11. Edward, S.; Nyerere, N. Modelling typhoid fever with education, vaccination and treatment. *Eng. Math.* **2016**, *1*, 44–52.
12. Karunditu, J.W.; Kimathi, G.; Osman, S. Mathematical modeling of typhoid fever disease incorporating unprotected humans in the spread dynamics. *J. Adv. Math. Comput. Sci.* **2019**, *32*, 1–11. [CrossRef]
13. Mutua, J.M.; Wang, F.B.; Vaidya, N.K. Modeling malaria and typhoid fever co-infection dynamics. *Math. Biosci.* **2015**, *264*, 128–144. [CrossRef]
14. Tilahun, G.T.; Makinde, O.D.; Malonza, D. Co-dynamics of pneumonia and typhoid fever diseases with cost effective optimal control analysis. *Appl. Math. Comput.* **2018**, *316*, 438–459. [CrossRef]
15. González-Guzmán, J. An epidemiological model for direct and indirect transmission of typhoid fever. *Math. Biosci.* **1989**, *96*, 33–46. [CrossRef] [PubMed]
16. Mushanyu, J.; Nyabadza, F.; Muchatibaya, G.; Mafuta, P.; Nhawu, G. Assessing the potential impact of limited public health resources on the spread and control of typhoid. *J. Math. Biol.* **2018**, *77*, 647–670. [CrossRef]
17. Shaikh, A.S.; Nisar, K.S. Transmission dynamics of fractional order Typhoid fever model using Caputo–Fabrizio operator. *Chaos Solitons Fractals* **2019**, *128*, 355–365. [CrossRef]
18. Mushayabasa, S. Modeling the impact of optimal screening on typhoid dynamics. *Int. J. Dyn. Control* **2016**, *4*, 330–338. [CrossRef]
19. Edward, S. A deterministic mathematical model for direct and indirect transmission dynamics of typhoid fever. *Open Access Libr. J.* **2017**, *4*, 75873. [CrossRef]
20. Tilahun, G.T.; Makinde, O.D.; Malonza, D. Modelling and optimal control of typhoid fever disease with cost-effective strategies. *Comput. Math. Methods Med.* **2017**, *2017*, 2324518. [CrossRef]
21. Peter, O.J.; Ibrahim, M.O.; Edogbanya, H.O.; Oguntolu, F.A.; Oshinubi, K.; Ibrahim, A.A.; Ayoola, T.A.; Lawal, J.O. Direct and indirect transmission of typhoid fever model with optimal control. *Results Phys.* **2021**, *27*, 104463. [CrossRef]
22. Musa, S.S.; Zhao, S.; Hussaini, N.; Usaini, S.; He, D. Dynamics analysis of typhoid fever with public health education programs and final epidemic size relation. *Results Appl. Math.* **2021**, *10*, 100153. [CrossRef]
23. Mondal, J. Influence of awareness programs by media in the typhoid fever: A study based on mathematical modeling. *J. Math. Model.* **2018**, *6*, 1–26.

24. Pitzer, V.E.; Bowles, C.C.; Baker, S.; Kang, G.; Balaji, V.; Farrar, J.J.; Grenfell, B.T. Predicting the impact of vaccination on the transmission dynamics of typhoid in South Asia: A mathematical modeling study. *PLoS Negl. Trop. Dis.* **2014**, *8*, e2642. [CrossRef] [PubMed]
25. Abboubakar, H.; Kombou, L.K.; Koko, A.D.; Fouda, H.P.E.; Kumar, A. Projections and fractional dynamics of the typhoid fever: A case study of Mbandjock in the Centre Region of Cameroon. *Chaos Solitons Fractals* **2021**, *150*, 111129. [CrossRef]
26. Sinan, M.; Shah, K.; Kumam, P.; Mahariq, I.; Ansari, K.J.; Ahmad, Z.; Shah, Z. Fractional order mathematical modeling of typhoid fever disease. *Results Phys.* **2022**, *32*, 105044. [CrossRef]
27. Abboubakar, H.; Racke, R. Mathematical modeling, forecasting, and optimal control of typhoid fever transmission dynamics. *Chaos Solitons Fractals* **2021**, *149*, 111074. [CrossRef]
28. Peter, O.; Ibrahim, M.; Oguntolu, F.; Akinduko, O.; Akinyemi, S. Direct and indirect transmission dynamics of typhoid fever model by differential transform method. *J. Sci. Technol. Educ.* **2018**, *6*, 167–177.
29. Pitzer, V.E.; Feasey, N.A.; Msefula, C.; Mallewa, J.; Kennedy, N.; Dube, Q.; Denis, B.; Gordon, M.A.; Heyderman, R.S. Mathematical modeling to assess the drivers of the recent emergence of typhoid fever in Blantyre, Malawi. *Clin. Infect. Dis.* **2015**, *61*, S251–S258. [CrossRef]
30. Syed, K.A.; Saluja, T.; Cho, H.; Hsiao, A.; Shaikh, H.; Wartel, T.A.; Mogasale, V.; Lynch, J.; Kim, J.H.; Excler, J.L.; et al. Review on the recent advances on typhoid vaccine development and challenges ahead. *Clin. Infect. Dis.* **2020**, *71*, S141–S150. [CrossRef]
31. Wang, W.; Zhao, X.Q. Threshold dynamics for compartmental epidemic models in periodic environments. *J. Dyn. Differ. Equ.* **2008**, *20*, 699–717. [CrossRef]
32. Tian, J.P.; Wang, J. Some results in Floquet theory, with application to periodic epidemic models. *Appl. Anal.* **2015**, *94*, 1128–1152. [CrossRef]
33. Zhang, F.; Zhao, X.Q. A periodic epidemic model in a patchy environment. *J. Math. Anal. Appl.* **2007**, *325*, 496–516. [CrossRef]
34. Smith, H.L.; Waltman, P. *The Theory of the Chemostat: Dynamics of Microbial Competition*; Cambridge University Press: Cambridge, UK, 1995.
35. Zhao, X.Q. *Dynamical Systems in Population Biology*, 2nd ed.; Springer: New York, NY, USA, 2017.
36. Zhao, X.Q. *Dynamical Systems in Population Biology*; Springer: New York, NY, USA, 2003.
37. Geoba.se. Population Website. Available online: http://www.geoba.se/country.php?cc=TW&year=2023 (accessed on 1 June 2023).
38. Taiwan National Infectious Disease Statistics System. Typhoid Fever. Available online: https://nidss.cdc.gov.tw/en/SingleDisease.aspx?dc=1&dt=2&disease=002 (accessed on 1 June 2023).
39. McKay, M.D.; Beckman, R.J.; Conover, W.J. Comparison of three methods for selecting values of input variables in the analysis of output from a computer code. *Technometrics* **1979**, *21*, 239–245.
40. Mitchell, C.; Kribs, C. A comparison of methods for calculating the basic reproductive number for periodic epidemic systems. *Bull. Math. Biol.* **2017**, *79*, 1846–1869. [CrossRef]
41. Hornick, R.; Greisman, S.; Woodward, T.; DuPont, H.; Hawkins, A.; Snyder, M. Typhoid fever: Pathogenesis and immunologic control. *N. Engl. J. Med.* **1970**, *283*, 739–746. [CrossRef]
42. Wain, J.; Diep, T.S.; Ho, V.A.; Walsh, A.M.; Hoa, N.T.T.; Parry, C.M.; White, N.J. Quantitation of bacteria in blood of typhoid fever patients and relationship between counts and clinical features, transmissibility, and antibiotic resistance. *J. Clin. Microbiol.* **1998**, *36*, 1683–1687. [CrossRef]
43. Mushayabasa, S.; Bhunu, C.P.; Mhlanga, N.A. Modeling the transmission dynamics of typhoid in malaria endemic settings. *Appl. Appl. Math. Int. J. (AAM)* **2014**, *9*, 9.
44. Cho, J.C.; Kim, S.J. Viable, but non-culturable, state of a green fluorescence protein-tagged environmental isolate of Salmonella typhi in groundwater and pond water. *FEMS Microbiol. Lett.* **1999**, *170*, 257–264. [CrossRef] [PubMed]
45. Saltelli, A. Sensitivity analysis for importance assessment. *Risk Anal.* **2002**, *22*, 579–590. [CrossRef]
46. Arriola, L.; Hyman, J.M. Sensitivity analysis for uncertainty quantification in mathematical models. In *Mathematical and Statistical Estimation Approaches in Epidemiology*; Springer: Dordrecht, The Netherlands, 2009; pp. 195–247.
47. Van den Driessche, P.; Watmough, J. Reproduction numbers and sub-threshold endemic equilibria for compartmental models of disease transmission. *Math. Biosci.* **2002**, *180*, 29–48. [CrossRef]
48. Centers for Disease Control and Prevention. Vaccine Information Statements (VISs). Typhoid VIS. Available online: https://www.cdc.gov/vaccines/hcp/vis/vis-statements/typhoid.html (accessed on 1 June 2023).
49. Irena, T.K.; Gakkhar, S. A dynamical model for HIV-typhoid co-infection with typhoid vaccine. *J. Appl. Math. Comput.* **2021**, *67*, 641–670. [CrossRef]